

EXPLORATION OF A NEW AFFORDABLE THERMAL PROTECTION SYSTEM
UTILIZING NEEDLE-PUNCHED (2.5D) FABRIC COMPOSITES

by

Ryan McDermott, B.S.

A thesis submitted to the Graduate Council of
Texas State University in partial fulfillment
of the requirements for the degree of
Master of Science
with a Major in Manufacturing Engineering
August 2018

Committee Members:

Jitendra S. Tate / Chair

Bahram Asiabanpour / Co-Chair

Joseph Koo / Co-Chair

COPYRIGHT

by

Ryan McDermott

2018

FAIR USE AND AUTHOR'S PERMISSION STATEMENT

Fair Use

This work is protected by the Copyright Laws of the United States (Public Law 94-553, section 107). Consistent with fair use as defined in the Copyright Laws, brief quotations from this material are allowed with proper acknowledgement. Use of this material for financial gain without the author's express written permission is not allowed.

Duplication Permission

As the copyright holder of this work I, Ryan McDermott, authorize duplication of this work, in whole or in part, for educational or scholarly purposes only.

ACKNOWLEDGMENTS

This thesis is the conclusion of three years of learning and research at Texas State University. I returned to school after working professionally for more than ten years with a desire to strengthen my technical expertise. I selected Texas State because of its emphasis on additive manufacturing, composites, and hands-on teaching methods. My experience in the Master's program has been incredibly fulfilling, and I feel extremely well-equipped to join the workforce as an engineer. I am extremely thankful to the guidance and mentoring Dr. Tate has provided me throughout the process.

I returned to school, a full-time employee, a father of one, and we had our second child shortly after I started. I am extremely grateful to my wife and family for being incredibly supportive through the long nights and absent days. Dr. Koo and Dr. Asiabanpour have been extremely supportive throughout the process and I'm thankful for their guidance.

A number of individuals were instrumental in helping in different stages of the project: Esmer Trevino, Tim Kuntz, Elijah Danielson, Shelby Vasconcellos Murphy, Sagar Navle, and Swayam Shree of Texas State; Dr. Koo's research group from UT Austin; Jon Langston, Dr. Hao Wu, and Will Fahy; and Dr. Jarrod Buffy of Techneglas.

TABLE OF CONTENTS

| | Page |
|---|-------------|
| ACKNOWLEDGEMENTS..... | iv |
| LIST OF TABLES..... | vii |
| LIST OF FIGURES..... | ix |
| ABSTRACT..... | xiii |
| CHAPTER | |
| I. INTRODUCTION..... | 1 |
| Background Information..... | 3 |
| Ablation Mechanisms in TPS..... | 3 |
| Reinforcement Materials in Thermal Protection Systems..... | 4 |
| Glass fibers..... | 5 |
| Carbon/graphite fibers..... | 6 |
| Aramid Fibers..... | 7 |
| Reinforcement Architectures in Thermal Protection Systems..... | 7 |
| Resin Systems in Thermal Protection Systems..... | 12 |
| Composites Manufacturing for Thermal Protection Systems..... | 13 |
| Goals and Objectives..... | 15 |
| II. MANUFACTURING..... | 16 |
| Material System..... | 16 |
| Needle-Punching of Silica Preform..... | 16 |
| VARTM Modified with Pressure to Control Thickness..... | 19 |
| III. PERFORMANCE EVALUATION..... | 27 |
| Mechanical Testing..... | 27 |
| Thermal Properties Testing..... | 28 |
| TGA Experiment..... | 28 |
| Ablation Testing..... | 28 |

| | |
|---|----|
| IV. RESULTS AND DISCUSSION..... | 31 |
| Mechanical Properties Testing..... | 31 |
| Interlaminar Shear Strength..... | 31 |
| Flexural Test..... | 31 |
| Tension Properties Testing..... | 31 |
| Thermal Properties Testing..... | 33 |
| TGA Results..... | 33 |
| OTB Results..... | 35 |
| Molding Compound, 2D, and 2.5D Comparison..... | 36 |
| Comparison of 2.5D Formulations with Increasing Needle-Punching..... | 42 |
| Microstructural Analysis using SEM..... | 47 |
| Analysis of Variance..... | 50 |
| V. CONCLUSIONS..... | 52 |
| APPENDIX SECTION..... | 55 |
| REFERENCES..... | 59 |

LIST OF TABLES

| Table | Page |
|--|-------------|
| 1. Composite thermal protection systems | 1 |
| 2. Fiber reinforcement properties..... | 5 |
| 3. 2D composites..... | 8 |
| 4. Needle punched (2.5D) composites | 9 |
| 5. 3D composites..... | 10 |
| 6. Ablative polymer characteristics..... | 11 |
| 7. Composite manufacturing techniques..... | 14 |
| 8. Preliminary resin reduction and VARTM experiments | 21 |
| 9. Ablative panel experiments..... | 23 |
| 10. Mechanical testing panel experiments | 25 |
| 11. ILSS properties summary | 31 |
| 12. Flexural properties summary | 32 |
| 13. Tensile properties summary | 33 |
| 14. Summary of test composites | 36 |
| 15. Summary of collected OTB data for molding compound, 2D, and 2.5D | 39 |
| 16. Summary of collected OTB data for 2.5D composites with increasing needle-punching time (10 min, 20 min, and 40 min) | 45 |
| 17. P-Values from ANOVA for each mechanical test comparison | 50 |
| 18. P-Values from ANOVA for OTB tests on MC, 2D, and 2.5D | 51 |

| | |
|---|----|
| 19. P-Values from ANOVA for OTB tests on 10 min, 20 min, and 40 min | 51 |
| 20. Comparison of mechanical and ablation properties of MX-2600, 2D, and 2.5D | 54 |

LIST OF FIGURES

| Figure | Page |
|--|------|
| 1. Peak heat flux of various NASA missions..... | 3 |
| 2. Ablation mechanisms..... | 4 |
| 3. TGA of ablative polymers | 12 |
| 4. Cross-sectional view of a solid rocket nozzle..... | 13 |
| 5. Thesis focus | 15 |
| 6. Properties of Dyna-Glas UHTR resin..... | 16 |
| 7. 36-inch needle-punching machine | 17 |
| 8. Simple lap-shear test..... | 17 |
| 9. Needle-punching screening..... | 18 |
| 10. Timing test on woven silica | 18 |
| 11. Weight supported on each side | 18 |
| 12. Needle-punched preform | 19 |
| 13. Resin reduction experiments..... | 20 |
| 14. Final samples from experiments 1 through 6..... | 22 |
| 15. Short beam testing..... | 27 |
| 16. Oxyacetylene test bed at UT Austin | 29 |
| 17. Instrumentation on an oxyacetylene test bed at UT Austin | 29 |
| 18. Sample being tested on the oxyacetylene test bed..... | 29 |

| | |
|--|----|
| 19. Needle-punched ablation samples..... | 30 |
| 20. (a) Representative interlaminar shear and (b) cumulative interlaminar shear test results..... | 31 |
| 21. Representative flexural test results | 32 |
| 22. Flexural (a) strength and (b) modulus results | 32 |
| 23. Tensile (a) strength and (b) modulus results..... | 33 |
| 24. (a) TGA and (b) DrTGA for neat resin systems | 34 |
| 25. (a) TGA in N ₂ and (b) TGA in air..... | 35 |
| 26. (a) DrTGA in N ₂ and (b) DrTGA in air | 35 |
| 27. (a) Density and (b) wt% resin in composites | 36 |
| 28. (a) Peak heat-soaked temperature and (b) backside temperature over time for 2D and 2.5D ablatives..... | 37 |
| 29. Post-test sample (left) and pre-test sample (right) | 38 |
| 30. (a) Recession rate (mm/s) and (b) mass loss rate (g/s) of different ablatives | 38 |
| 31. (a) Mass loss (%) and (b) char yield (%) of different ablatives..... | 39 |
| 32. Surface temperature over time for 2D and 2.5D ablatives..... | 40 |
| 33. Infrared imagery of representative molding compound, 2D, and 2.5D samples | 41 |
| 34. (a) High-definition imagery of representative molding compound, 2D, and 2.5D samples and (b) ply burn-through over time for 2D and 2.5D representative samples | 42 |
| 35. (a) Density and (b) wt% resin in 2.5D composites with increasing needle-punching time (10 min, 20 min, and 40 min)..... | 43 |

| | |
|--|----|
| 36. (a) Peak heat-soaked temperature and (b) backside temperature over time for 2.5D composites with increasing needle-punching time (10 min, 20 min, and 40 min) | 43 |
| 37. (a) Recession rate and (b) mass loss rate (g/s) in 2.5D composites with increasing needle-punching time (10 min, 20 min, and 40 min) | 44 |
| 38. (a) Mass loss (%) and (b) char yield (%) in 2.5D composites with increasing needle-punching time (10 min, 20 min, and 40 min)..... | 45 |
| 39. Surface temperature over time for 2.5D ablatives with increasing needle-punching time (10 min, 20 min, and 40 min) | 46 |
| 40. Infrared imagery of representative 2.5D samples with increasing needle-punching time (10 min, 20 min, and 40 min) | 46 |
| 41. High-definition imagery of representative 2.5D samples with increasing needle-punching time (10 min, 20 min, and 40 min)..... | 47 |
| 42. Scanning electron micrographs of 2D and 2.5D composites showing the (a) 2D composite cross-section, (b) 2.5D composite cross-section, (c) fiber breakage in the 2.5D composite, and (d) randomly ordered non-woven silica mat..... | 48 |
| 43. Scanning electron micrographs of 2.5D ablative composites showing the (a) entire cross-section, (b) char layer, (c) heat affected zone, and (d) virgin layer..... | 49 |

ABSTRACT

Thermal protection systems (TPS) designed for solid rocket motors (SRMs) and reentry vehicles employ ablative composites. Phenolic and cyanate ester are state-of-the-art (SOTA) resin systems used in many of the ablative composites today, including MX-2600 from Cytec Solvay Group. While these ablatives have worked well, more demanding requirements drive the need for affordable lightweight advanced composites capable of handling high heat fluxes with less mass loss. These advanced ablative composites result in lighter heat shields and solid rocket motors, increasing payload capabilities of rockets and missiles. Molding compound made of aerospace grade 99% SiO₂ fabric and polysiloxane resin showed considerable improvement over MX-2600 in ablative properties in recent studies. Also, to meet increased mechanical strength demands, NASA recently developed an ablative composite using a 3D quartz woven material designed for the Orion spacecraft. While 3D woven composites provide excellent out-of-plane mechanical and ablation properties, they are very expensive, which limits their application. This research explores needle-punched silica fabric, sometimes referred to as 2.5D, which provides similar out-of-plane mechanical benefits to 3D woven composites in a more flexible VARTM manufacturing process at a much lower cost. The needle-punched silica fabric was infiltrated with polysiloxane resin, and mechanical tests were performed. The needle-punched composites showed a 181% increase in flexural strength, a 27% increase in interlaminar shear strength, and a 2% increase in tensile strength. In ablation tests, the 2.5D out-performed the 2D laminate in char yield, mass

loss, and recession rate; and in char yield and mass loss (%), the 2.5D out-performed the industry standard MX-2600 molding compound. The increased out-of-plane strength and char yield make it a promising and affordable candidate for ablation performance with enhanced mechanical properties.

Key Words: Ablation, thermal protection systems, needle punched, 2.5D, high-temperature, and polysiloxane

I. INTRODUCTION

A Thermal Protection System (TPS) serves as the boundary between high heat fluxes that would otherwise compromise the integrity of a spacecraft and critical systems.

These materials are also widely used as thermal protection in internal components of rocket motors or heat shields of aerodynamic surfaces that protect the valuable payload of missiles, space probes, or space vehicles [1]. Thermal protection systems are created using two categories of materials – ablative or non-ablative. Non-ablative materials, such as the ceramic tiles on the space shuttle re-radiate heat to insulate structural components and do not degrade during the heating process, whereas ablative materials predictably deteriorate throughout the heating process while insulating [1]. As shown in Table 1, each thermal protection material has a specific application based on its cost, weight, mechanical, and insulation properties.

Table 1. Composite thermal protection systems [2].

| Function | Material | Remarks |
|---|--|--|
| Heat sink and heat-resistant material at inlet and throat section of the solid rocket motor. Severe thermal environment and high-velocity gas, with erosion. | Carbon or Kevlar fiber cloth with phenolic or plastic resins | Sensitive to fiber orientation. Ablative materials Used with large rocket motor throats |
| | Carbon-carbon | Three- or four-dimensional interwoven filaments, strong, expensive, limited to 3,300°C (6,000°F) |
| Insulator (behind heat sink or flame barrier); not exposed to flowing gas | Ablative plastics, with fillers of silica or Kevlar, phenolic resins | Want low conductivity, good adhesion, ruggedness, erosion resistance; can be filament wound or impregnated cloth layup with subsequent machining |

Table 1 continued. Composite thermal protection systems [2].

| | | |
|---|---|--|
| Flame barrier (exposed to hot low-velocity gas) | Ablative plastics (same as insulators but with less filler) | Lower cost than carbon-carbon; better erosion resistance than many insulators |
| | Carbon, Kevlar, or silica fibers with phenolic or epoxy resin | Cloth or ribbon layups; woven and compressed, glued to the housing |
| | Carbon-carbon | Higher temperature than others, three-dimensional weave or layup |
| Nozzle exit cone | Ablative plastics with metal housing structure | Heavy, limited duration; cloth or woven ribbon layups, glued to the housing |
| | Carbon-carbon, may need gas seal | Radiation cooled, higher allowable temperature than metals; two or three-dimensional weave, strong, often porous |

Current advanced thermal protection systems use state of the art (SOTA) resins, such as SC-1008 phenolic with silica or carbon fiber reinforcement [3], however, as shown in Figure 1, the range of heat fluxes endured by TPS systems vary widely. The Galileo mission to Jupiter in 1995 had a peak heating rating of 30 kW/cm^2 [4]. A report from NASA-Ames in 2003 stated that future probes to Jupiter that are not equatorial would involve higher heating rates and a carbon phenolic TPS system would not be suitable due to its TPS mass fraction (high weight to ablation resistance). “A new, robust and efficient TPS is required for such probes” [5]. Further, space companies are striving to develop reusable rockets and space vehicles such as the Dragon by SpaceX. In 2013, SpaceX developed a PICA-X heat shield capable of enduring temperatures up to $3,000^\circ\text{F}$ during re-entry [6].

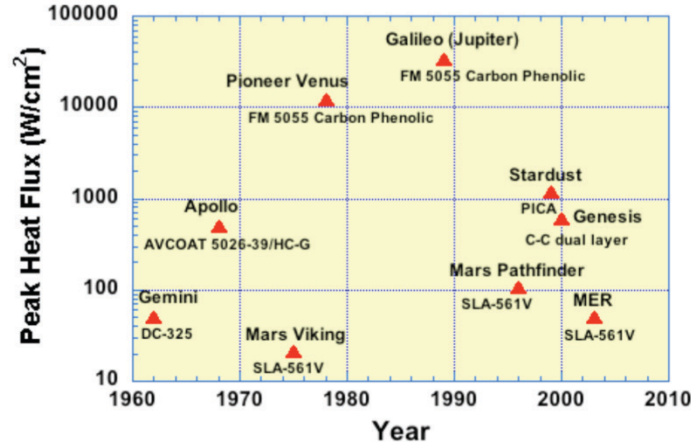


Figure 1. Peak heat flux of various NASA missions [5].

Background Information

Ablation Mechanisms in TPS. Ablative material predictively degrades over time when exposed to external heat fluxes, such as solid rocket motor exhaust or reentry gases at high speed. Figure 2 shows the sequential erosion of the ablative that occurs when exposed to high heat fluxes. The polymer first experiences heat transfer through conduction and as the material heats up, its thermal expansion causes the material to expand slightly. The pyrolysis layer then begins to form as the polymer starts to decompose under the high temperature. As the polymer rises in temperature, typically between 250°C and 600°C, the pyrolysis layer progresses through the thickness of the ablative composite. After the polymer decomposes and the pyrolysis zone retreats deeper into the ablative composite a porous char layer is left behind [7, 8]. The char layer is critical to the performance of an ablative. It acts as an insulator, slowing the diffusion of heat to the pyrolysis layer and limits the amount of oxygen available for exothermic reactions in the virgin material. The char layer also protects the virgin material from direct exposure to flames, and the release of gases from the pyrolysis layer are slowed as they traverse the porous char layer which causes the ablative composite to cool [9]. The

polymer plays a crucial role in establishing a char layer, but without fiber reinforcement, it will erode under the harsh conditions [8]. The Koo Research Group at UT Austin has investigated a high-temperature polysiloxane resin produced by Techneglas LLC, UHTR, that has a high char yield, that is indicative of a material that will perform well as an ablative [9]. During the ablation process, the char layers are exposed to high heat fluxes as well as gases flowing parallel to the material. As the polymer matrix degrades, a typical 2D laminate composite is subject to delamination, causing the protective char layer to erode quickly. Mechanical testing of the needle-punched composites shows enhanced mechanical performance and higher resistance to mechanical shear. The improved out-of-plane mechanical properties, combined with the high char yield of the high-temperature polysiloxane resin make a needle-punched silica polysiloxane composite a good candidate for ablation.

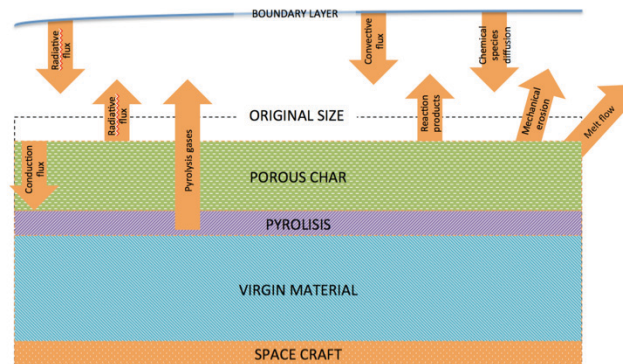


Figure 2. Ablation mechanisms [1] [5].

Reinforcement Materials in Thermal Protection Systems.

Reinforcements provide the strength, stiffness, and mechanical properties of the final composite part, and significantly contribute to the coefficient of thermal expansion and conductivity. Fiber density and length have the most effect on mechanical properties, increasing tensile strength, modulus of elasticity, flexural strength, and elongation. Weight is a critical factor in fiber selection for aerospace applications where it can cost as much as

\$10,000/lb to launch a satellite into space. Fibers that are commonly used in ablative applications include silica and carbon [10]. The fibers and their properties are shown in Table 2.

Table 2. Fiber reinforcement properties [10].

| Fiber Type | Density, g/cc | Tensile Strength, ksi | Tensile Modulus, Msi | Elongation at Break, % |
|--|---------------|-----------------------|----------------------|------------------------|
| Glass (E-Glass) | 2.5 | 500 | 10 | 4.9 |
| Glass (S-Glass) | 2.5 | 665 | 12 | 5.7 |
| Carbon/graphite (standard modulus) | 1.8 | 600 | 33 | 1.6 |
| Carbon/graphite (intermediate modulus) | 1.8 | 780 | 40 | 1.8 |
| Carbon/graphite (ultra-high modulus) | 1.9 | 500 | 64 | 0.5 |
| Aramid (high toughness) | 1.4 | 523 | 12 | 4.0 |
| Aramid (high modulus) | 1.4 | 580 | 19 | 2.8 |
| Aramid (ultra-high modulus) | 1.4 | 494 | 27 | 2.0 |

Glass Fibers. Continuously formed glass fibers for reinforcement were made manufactured as early as 1937. They initially were used in airplane, auto, and boat parts because of their lightweight and high strength. Glass fibers consist mostly of silica (SiO_2) and have other materials to determine specific properties and workability. The five types of glass fibers used when creating composite materials are E-glass, S-glass, C-glass, silica, and quartz.

- E-glass – Known for value, E-glass fibers have good strength and low cost and are used the most in composite applications.
- S-glass – Stronger than E-glass by 35% and maintains mechanical properties better at higher temperatures.
- C-glass – Between E-glass, S-glass, and C-glass, C-glass has the highest coefficient of thermal expansion and lowest softening point.

- Silica – Non-conductive with a very high melting point.
- Quartz – Made from quartz, it has lower strength and density but a better softening point temperature and electrical transparency [10].

Carbon/graphite fibers. In the 1950s carbon fibers were developed to meet the demand for even stronger reinforcement materials than glass fibers. Three methods are used to create carbon fibers – polyacrylonitrile (PAN), pitch, and rayon.

- PAN fibers – Low cost, with a standard modulus.
- Pitch fibers – High modulus with good thermal conductivity.
- Rayon fibers – Typically only used in legacy applications.

Carbon fibers, mixed with the appropriate matrix material have high strength, stiffness, and toughness while maintaining a low weight. Carbon fibers weaknesses are that they are brittle, are susceptible to impact, oxidation, and have low strength in compression. As cost has decreased, the applications where carbon fibers are used have increased significantly. Carbon fibers are used where high strength to weight ratio is important, such as aircraft, automobiles, and spacecraft. They are also used in thermal applications, such as heat shields, space structures, and computer applications [10]. Carbon fibers are used in industry standard MX-4926 thermal protection systems, but they are not ideal for oxidizing environments.

Aramid Fibers. Kevlar, a version of aramid produced by Dupont® is a household name, used in body protection applications. Aramid fibers were introduced in 1971 and used as reinforcement in tires and other products that were made of rubber. Today they are widely used in ballistic protection applications. Aramids are produced and available in three forms – high toughness, high modulus, and ultra-high modulus and they have a

lower density than glass and carbon fibers while maintaining a strength and stiffness between that of glass and carbon fibers. Aramid fibers are used in bulletproof vests, ship and vehicle armor, and battlefield shelters. They are also employed on surfaces that have a high risk of impact damage, such as leading edges of airplanes [10].

Reinforcement Architectures in Thermal Protection Systems. Fibers for ablative composites are available in three different architectures - 2D, needle-punched (also referred to as 2.5D), and 3D. Tables 3-5 describe the technology currently available for use in the textile and composites industry and their associated advantages and disadvantages. The toughness of the char layer contributes to an ablative materials ability to withstand high heat fluxes with less recession over time. Recently, to meet new mechanical strength demands, NASA developed an ablative composite using a 3D quartz woven material. As shown in Table 5, 3D woven composites provide excellent out-of-plane mechanical and ablation properties; however, they are expensive to produce, which limits their application. As shown by Meng et al., combining the superior drape and stretch capabilities of a harness-weave silica fabric with needle-punching has the ability to produce a composite that has improved out-of-plane mechanical properties while retaining the cost and strength characteristics of a 2D fabric [11].

Table 3. 2D composites [12] [13] [10].

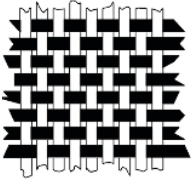
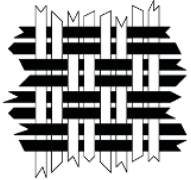
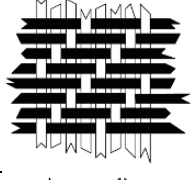
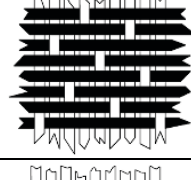
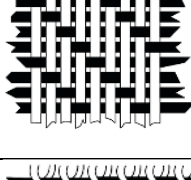
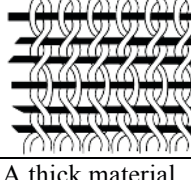
| Technique | Cost | Comments | Advantages | Disadvantages |
|------------------------|------|---|---|---|
| 2D Composite | | | | |
| Plain weave | Low |  | <ul style="list-style-type: none"> • Best fabric stability and firmness • Best resistance to in-plane shear | <ul style="list-style-type: none"> • Limited to flat laminates, circuit boards, and covering other structures. |
| Basket weave | Low |  | <ul style="list-style-type: none"> • Flat and strong compared to plain weave • Better drape than plain weave | <ul style="list-style-type: none"> • Prone to defects at crimp points |
| Twill weave | Low |  | <ul style="list-style-type: none"> • Better drape and wet-out than plain weave | <ul style="list-style-type: none"> • Lower stability than plain weave |
| Satin or harness weave | Low |  | <ul style="list-style-type: none"> • Great drape • Ability to stretch in any direction | <ul style="list-style-type: none"> • Lower stability than plain weave • Wetting and removing air can be difficult |
| Crowfoot weave | Low |  | <ul style="list-style-type: none"> • Great drape with the ability to fit spherical shapes • Stronger in the warp direction than plain weave | <ul style="list-style-type: none"> • Wetting and removing air can be difficult |
| Leno weave | Low |  | <ul style="list-style-type: none"> • Fabric is heavy allowing for fast ply buildup • Good for inner structural layers | |
| Woven Roving | Low | A thick material designed using one of the above weave patterns loosely. | <ul style="list-style-type: none"> • Thick for easy buildup of reinforcement sections | |
| Veil | Low | A tightly woven material using one of the above weaves. | <ul style="list-style-type: none"> • Better aesthetics and smoothness • Barrier between the buildup material and the outside of the part | |
| Mats | Low | Consist of either continuous or chopped fibers | <ul style="list-style-type: none"> • Easy application, such as spray up • Continuous mats are often used in veil applications | <ul style="list-style-type: none"> • Lower strength characteristics than woven |

Table 4. Needle punched (2.5D) composites [12] [13] [10].

| Technique | Cost | Comments | Advantages | Disadvantages |
|------------------------|-------------|--|---|--|
| Needle Punched Fabrics | | | | |
| Needle-punching | Low | Complex shapes can be produced inexpensively | <ul style="list-style-type: none"> • Complex shapes • Higher delamination resistance • Higher interlaminar fracture toughness • Higher interlaminar impact damage tolerance | <ul style="list-style-type: none"> • The process degrades the in-plane mechanical properties • Many properties are still not fully understood – effects of high speed needle punching process, durability and long-term environmental aging properties, and strength and fatigue performance |

Table 5. 3D composites [12] [13] [10].

| Technique | Cost | Comments | Advantages | Disadvantages |
|-------------------|--------|--|--|---|
| 3D Fabrics | | | | |
| Weaving | Medium | Expensive and difficult to manufacture | <ul style="list-style-type: none"> • Higher delamination, ballistic, and impact damage resistance • Higher tensile strain-to-failure values • Higher interlaminar toughness | <ul style="list-style-type: none"> • Expensive and challenging to manufacture • Lower tension, compression, shear and torsion properties • Many properties are still not fully understood – durability and long-term environmental aging properties and strength and fatigue performance |
| Braiding | High | Expensive and not capable of complex shapes | <ul style="list-style-type: none"> • Higher delamination and impact damage resistance • Excellent crash properties | <ul style="list-style-type: none"> • Not capable of producing complex forms • Lower stiffness and strength • Many properties are still not fully understood – durability and long-term environmental aging properties and strength and fatigue performance |
| Knitting | Medium | Capable of producing more complex shapes. Can be manufactured on existing automation machines. Not capable of making thick shapes. | <ul style="list-style-type: none"> • Higher delamination and impact damage resistance • Higher crash properties | <ul style="list-style-type: none"> • Lower stiffness and strength properties • Many properties are still not fully understood – strength and fatigue performance • Soft and hard spots in the final composite |
| Stitching | Medium | Expensive and not capable of producing complex shapes. | <ul style="list-style-type: none"> • Higher impact, delamination, ballistic, and blast strength • Higher mechanical properties | <ul style="list-style-type: none"> • Difficulty forming – thick preforms and curved or complex shapes • Many properties are still not fully understood – durability and long-term environmental aging properties and strength and fatigue performance |

Resin Systems in Thermal Protection Systems. Many solid rocket motor nozzles in use today utilize phenolic resin. For example, MX-4926 and MX-2600 produced by Cytec Solvay Group utilizes a phenolic matrix with carbon and silica reinforcement, respectively [7]. Phenolic resin is also widely used commercially in automotive and home applications in combination with low-cost fillers that reduce its high shrinkage rate. Phenolic resin is often selected because of its incredible flammability resistance as well as the lack of smoke, toxicity, and flame spread produced by the resin. In protection scenarios, phenolic has low heat transfer and high thermal stability. These qualities have made it the resin system of choice for past thermal protection systems [10].

Boghozian et al. at NASA did a review of high-performance ablative polymers in 2015 to compare their qualities with phenolic resin. Table 6 below summarizes the characteristics of the resins and Figure 3 shows the results of the thermal gravimetric analysis, which provides a good indicator of a polymers resistance to high heat fluxes.

Table 6. Ablative polymer characteristics [14].

| | Decomposition Temp | Char yield | Advantages/Disadvantages |
|--------------------------|---------------------------|-------------------|--|
| Phenolic | 375°C | 49% | Well understood resin system, but brittle and susceptible to oxidation |
| Cyanate ester | 417°C | 56% | Resistant to water and radiation, high T_g |
| Polyimide | 529°C | 67% | High stability at temperatures below 400° C, high T_g , good mechanical properties |
| Polybenzoxazine | 294°C | 20% | High T_g and good resistance to moisture |
| Polybenzimidazole | 298°C | 52% | Not susceptible to oxidation and its mechanical properties are good. |

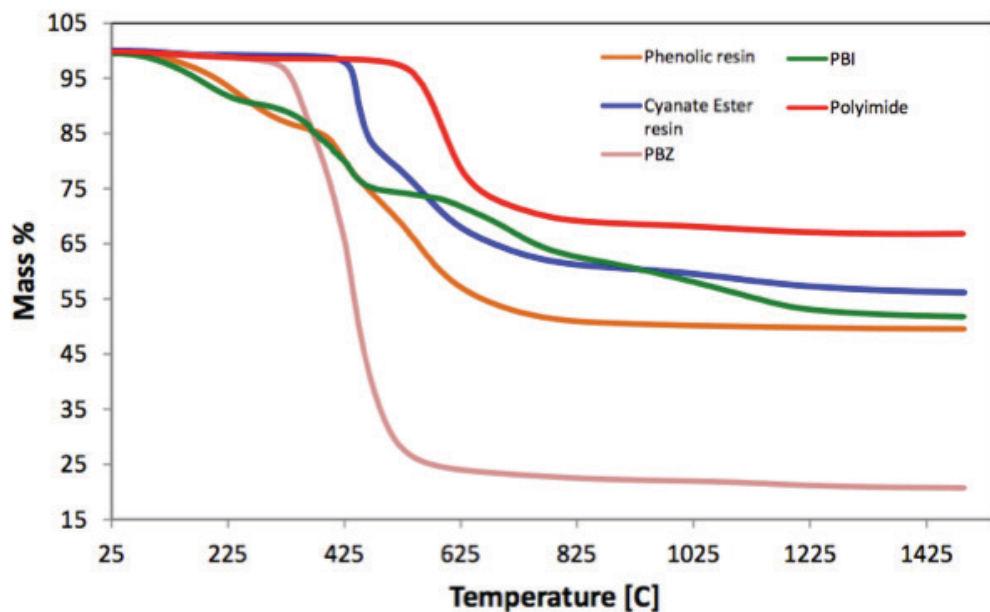


Figure 3. TGA of ablative polymers [14].

Fine ceramics, such as zirconia, alumina, and silicon carbide provide exceptional heat resistance as well. This is because many fine ceramics do not begin to melt until temperatures exceed 2,000°C making them ideal candidates for thermal protection systems [15]. Polysiloxane is a pre-ceramic polymer, meaning that when it is heated at sufficiently high temperatures it undergoes pyrolysis and converts to a ceramic [16]. This pyrolysis reaction typically occurs during ablation making a polysiloxane-based resin an excellent candidate for ablatives.

One such polysiloxane chemistry based resin, produced by Techneglas is designed for high-temperature applications ranging from 315° to 980°C. It has the capability of curing at low temperatures and exhibits good chemical resistance and produces little to no smoke when exposed to fire [3]. In a study carried out by the Schellhase et al., the neat polysiloxane resin system exhibited an 87% char yield, far

exceeding the char yield of SOTA resin systems as well as those measured by Boghozian et al. in Table 6 [9].

Composites Manufacturing for Thermal Protection Systems. The shape and integrity of an ablative rocket nozzle and throat is critical to a rocket motors ability to convert exhaust gas energy into predictable thrust throughout the firing phase. Generally, rocket nozzles are fabricated by wrapping a mandrel with a fiber reinforcement and resin “tape” similar to a prepreg [17]. Solid rocket nozzles can consist of a number of different materials as shown in Figure 4, making flexibility in manufacturing important.

Additionally, geometric changes to the exit cone can affect the final performance of the solid rocket motor, with some designs utilizing a straight-sided conical mandrel and others a contoured mandrel [18]. Several composite manufacturing technologies outlined in Table 7 are viable candidates for producing ablative solid rocket motor nozzles.

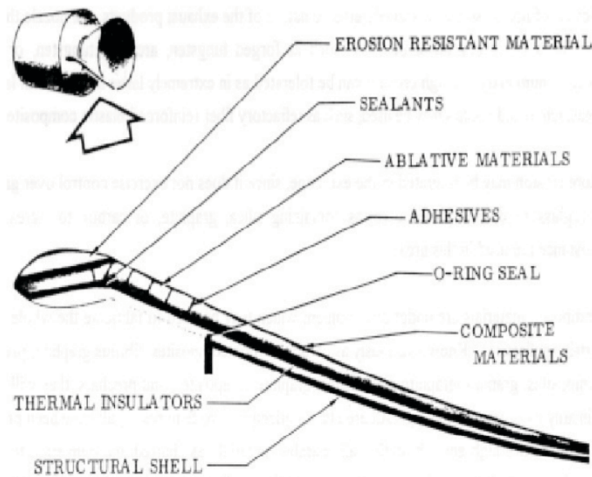


Figure 4. Cross-sectional view of a solid rocket nozzle [17].

Table 7. Composite manufacturing techniques [10].

| Technique | Advantages | Disadvantages |
|--|--|--|
| Wet-layup | Inexpensive and widely understood. Able to produce complex parts and contours. Molds can be changed rapidly because they don't need high tolerance machining. Low equipment cost. | Hard to produce high fiber volume parts consistently. Worker exposure to styrene emissions and higher labor costs. Typically curing of wet-layup is done at room temperature which isn't suitable for all resin systems. |
| Pre-preg | Predictable fiber volume ratios and repeatability. Can be automated with automatic tape layup robots. | Requires special freezer storage of pre-preg materials and not all fiber/matrix formulations are available. Only available in 2D fiber architectures. Typically cured in an autoclave which has a high equipment cost. |
| Compression molding | Produce consistent high fiber volume and high-density parts. Compatible with bulk molding compound (BMC), sheet molding compound (SMC) and pre-preg. | Requires robust precision molds that are expensive and are limited to simple shapes. Equipment cost is high, especially when producing large format parts. |
| Resin transfer molding (pressure injected) | High precision and fiber volume (55-65%) parts with easy repeatability. | Requires precision molds that cannot be changed and are expensive. RTM injection equipment cost is high. |
| Vacuum infusion or VARTM | Molding surface is similar to wet-layup and can be produced inexpensively and easily changed. High-quality surface finish with the ability to produce fiber volumes of 45-55%. Low equipment cost and flexibility in fiber and matrix choices. | Limited to low viscosity resin systems and it may require an in-depth understanding of resin flow for complex parts. |
| Filament winding | Quickly produce cylindrical objects in a highly repeatable manner. Wide resin and fiber compatibility. | High equipment cost and limited shapes. Low exterior surface quality. |

Based on this analysis of the manufacturing technologies, vacuum assisted resin transfer molding has the ability to meet the shape, density, and fiber volume requirements for ablative composites, and the Techneglas polysiloxane resin has a compatible viscosity.

Goals and Objectives

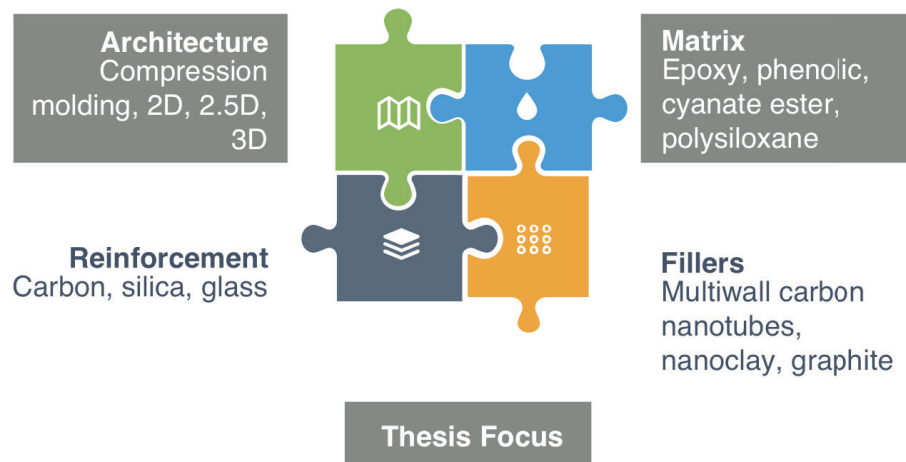


Figure 5. Thesis focus.

This research manipulates the architecture and matrix of the composite to explore the development of a novel thermal protection system capable of meeting the intense thermal demands experienced inside solid rocket motors. Typical thermal protection systems designed to withstand a high-heat flux require specialized and expensive manufacturing techniques specific to each part. It is expected that combining a low-cost needle-punching technique, promising new resin chemistry, and flexible VARTM process will yield an affordable high-performance thermal protection material.

II. MANUFACTURING

Material System

The polysiloxane resin used as the matrix in this research is Techneglas UHTR resin produced by Techneglas, LLC. The resin is shipped with 35 wt% isopropyl alcohol for dispersion and to prevent curing. The resin is cured with heat at or above 225°C at atmospheric pressure, and the physical properties of the uncured and cured resin are listed in Figure 6 below.

| Product Data | |
|---|------------------------|
| Uncured Dyna-Glas UHTR | |
| Appearance | Slightly cloudy liquid |
| Viscosity | 95 cPs |
| Percent of Solids | 65% |
| Odor (liquid) | Slight Solvent |
| V.O.C. | 368 g/L (3.07 lb/gal) |
| Specific Gravity | 1.05 |
| Pot Life at 25°C when catalyzed | 1-3 hours |
| Liquid Ignition Temperature | >300°C |
| Cured Dyna-Glas UHTR (Silica Fiber Mat) | |
| Resin content of FRP | 40-50% |
| Specific Gravity | 1.56 |
| Thermal Conductivity, k (300°C) | 0.68 W/(m-K) |
| Specific Heat Capacity, C_p (300°C) | 1.3 J/gK |
| Weight loss at 1000°C (silica fiber) | < 5% |
| Tensile Strength (ASTM D638) | 8,020 psi |
| Modulus of Elasticity, MOE (ASTM D638) | 1,570 ksi |
| Flexural Strength (ASTM D790) | 11,100 psi |
| Flexural Modulus (ASTM D790) | 1,330 ksi |
| Rockwell Hardness (ASTM D785-08, R Scale) | 83 |

Figure 6. Properties of Dyna-Glas UHTR resin.

Needle-Punching of Silica Preform

Joining the woven silica ply's in the z-direction was accomplished using an industrial 36-inch needle-punching machine, shown in Figure 7. An extensive needle-punching exploration was conducted on different materials with different needle-

punching parameters to determine the ideal conditions to produce the 2.5D ablative samples. Screening tests to observe different material types, weaves, and their compatibility with needle-punching were performed, and a simple dry lap-shear test pictured in Figure 8 was used. Six different materials were tested with the dry lap shear test and the results are reported in Figure 9. The fiberglass with a chopped strand mat backing performed the best of any materials. To understand how the woven silica would perform further testing was conducted by varying the amount of time the material was needle-punched as shown in Figures 10 and 11. With silica, a threshold of needle-punching needed to join the ply's together was observed; however, with 12 minutes of needle-punching, instead of failing in shear, the ply's completely broke down and tore. Based on the performance of the chopped strand mat fiberglass, it was determined that incorporating a non-woven or mat silica material into the final pre-form would greatly enhance the strength in the z-direction. Balanced with reducing the total amount of needle-punching necessary to avoid excessive damage to the woven ply's. Figure 12 shows a representative sample of the non-woven/woven hybrid preform after needle-punching.

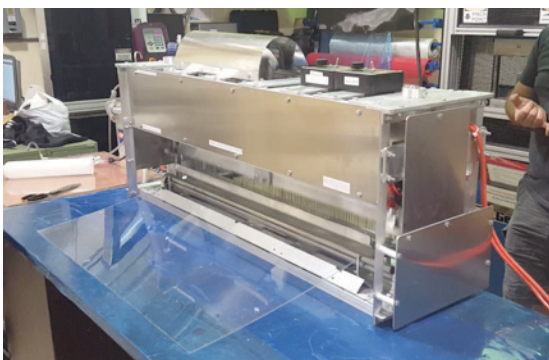


Figure 7. 36-inch needle-punching machine.

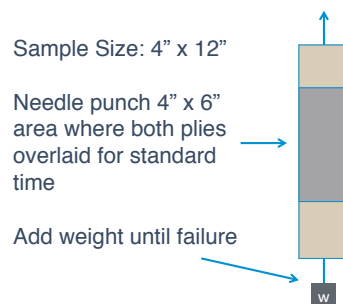


Figure 8. Simple lap-shear test.

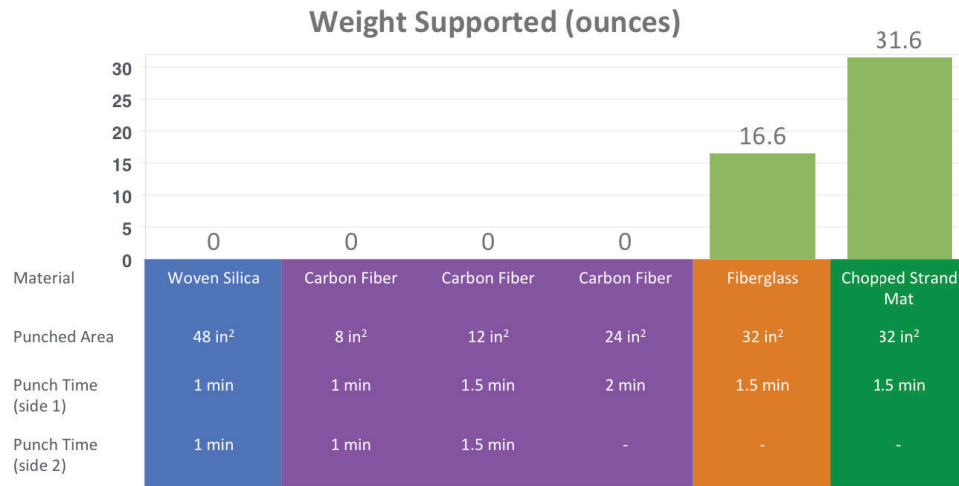


Figure 9. Needle-punching screening.



Figure 10. Timing test on woven silica.

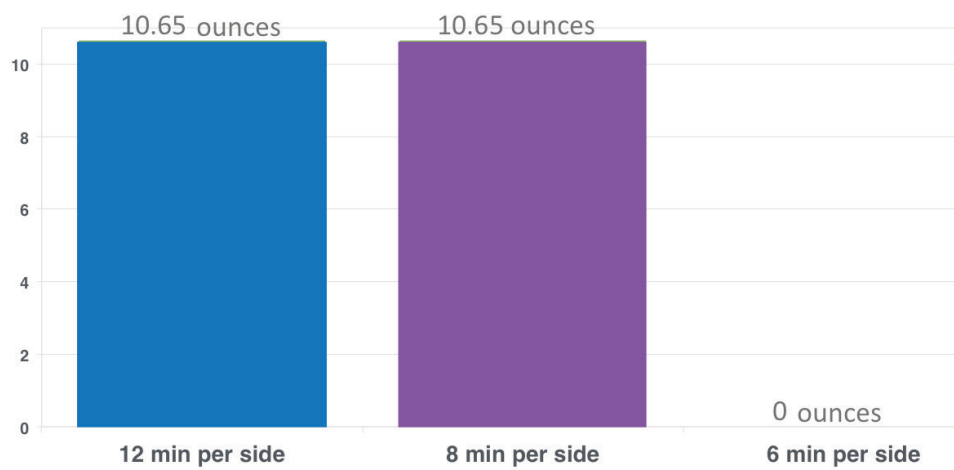


Figure 11. Weight supported on each side.



Figure 12. Needle-punched preform.

VARTM Modified with Pressure to Control Thickness

As-received, the Techneglas resin contains 35 wt% IPA which is not critical for the curing process but was problematic in the vacuum infusion process of experiment 1. The high IPA content made the viscosity of the resin too low and produced a composite panel with a low resin content. For experiment 2, to remove the IPA before the infusion process the team used a low heating rate of 80°C for 16-22 hours. The process did remove the IPA, but as shown in Figure 13, the application of heat caused the resin to bubble and harden on the surface. While it worked for the early experiments much of the resin was unusable and discarded as waste. Figure 14 shows the test panels produced in experiments 1-6. Experiments 1-5 did not produce a viable composite. After experiments 1-4, it was determined that the lowered vapor pressure of IPA under vacuum and the elevated temperature (110°C) caused the IPA to quickly boil off during infusion stopping the flow of the resin prematurely. For experiment 6, the infusion was conducted at room temperature, and for experiment 7, the manufacturer recommended reducing the IPA content using a vacuum at room temperature. This produced a resin that was in much better condition and flowed better during infusion. The final challenge with the infusion process was controlling the thickness of the test panels. In a typical VARTM setup, the thickness is established by the thickness of the woven preform depressed by

atmospheric pressure when under vacuum. The needle-punching process created a unique challenge. Needle-punching “fluffed” the material, causing the preform thickness to increase prior to infusion. To create an accurate comparison between 2D and 2.5D samples it was necessary to produce panels at the same thickness, and therefore, the same density. A compression press was selected to depress the samples to a specific thickness using spacers between two steel plates. The press was operated at a low-pressure and for cost savings, it could be replaced with a low-cost inflatable press bladder produced by Aero Tec Laboratories. Tables 8-10 provide details about each experiment’s procedures and results.

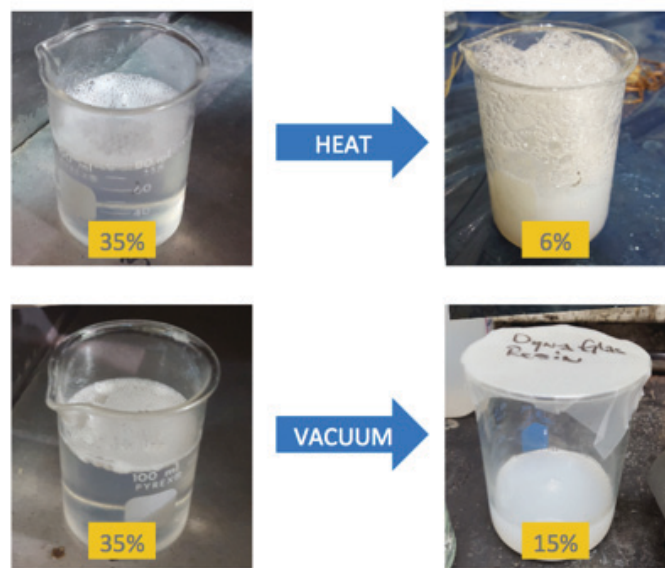


Figure 13. Resin reduction experiments.

Table 8. Preliminary resin reduction and VARTM experiments.

| | Purpose | Resin | Fiber | Infusion | Curing | Result |
|---|---|---|---|-----------------------------------|---|---|
| 1 | 1. Test resin flow 2. Effect of vacuum on the resin 3. Test heating pad for B-stage | 50 grams of resin as-received (35 wt. % IPA) | Four woven silica ply's stacked | At room temperature | 4hrs 20min @ 80°C | Not cured. Immediately delaminated. |
| 2 | 1.Reduce IPA prior to infusion. 2.Cure mold at elevated temperature | 76.3 grams of resin reduced to 14.2 wt. % IPA after 16:41hrs in the oven at 70-80°C | Four woven silica ply's stacked | Infused with heating pad at 110°C | In mold for 2 hrs. @ 150°C In oven for 2 hrs. @ 225°C | Infusion only progressed 1/3 of the way and then deformed during de-molding. |
| 3 | 1. Reduce IPA with heat prior to infusion. 2. Infuse with heat | 78g of resin reduced to 5.5 wt. % IPA after 19:41hrs inside oven at 85°C | Four woven silica ply's stacked | Infused at 110°C | No cure | No cure because resin flow stopped 20% of the way in. |
| 4 | Reduce IPA to 15 wt% | 81.93g of resin reduced to 14.7 wt. % IPA after 22:40hrs at 70-80°C | Four woven silica ply's stacked | Infused at 110°C. | No cure | No cure because resin flow stopped 25% of the way in. |
| 5 | Study effects of room temperature VARTM on the fluid flow. | 78.32g of resin reduced to 10.1 wt. % IPA after 21:15hrs at 70-80°C | Four woven silica ply's stacked | Infused at room temperature. | The entire cure was done in the bagging material at 150°C for 2 hours and then 225°C for 2 hours. | The resin flowed well but curing the panel in the bagging material was unnecessary. |
| 6 | Produce 2D and 2.5D panels large enough to cut ILSS samples from. | 150.17g of resin reduced to 15.7 wt. % IPA after 20:05hrs at 70-80°C | 2D - Four woven silica ply's stacked 2.5D - Four woven silica ply's needle-punched | Infused at room temperature. | Heating pad with vacuum at 150°C for 2 hours and then in the oven at 225°C for 2 hours. | Good resin flow, saturation, and curing. |

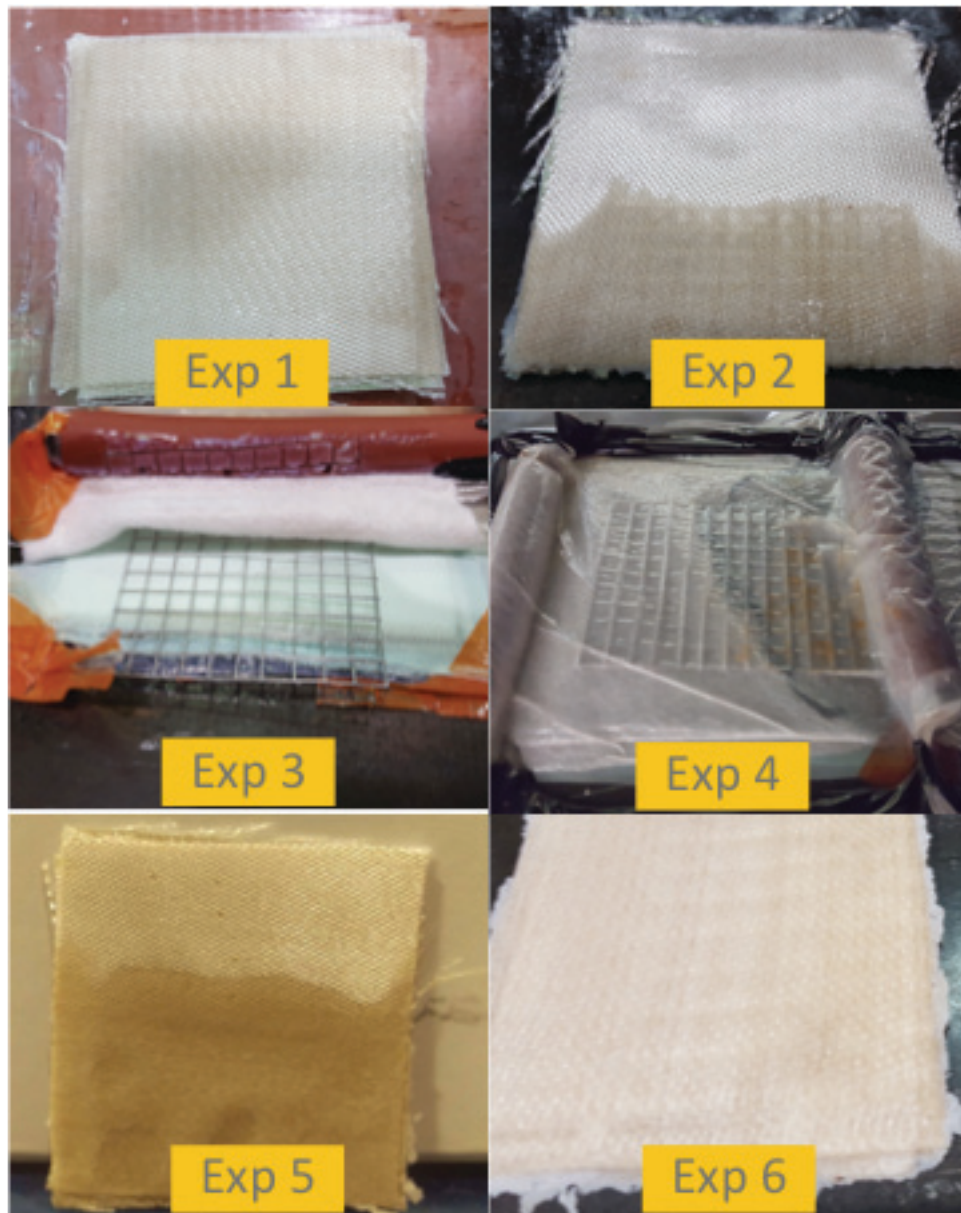


Figure 14. Final samples from experiments 1 through 6.

Table 9. Ablative panel experiments.

| | Purpose | Resin | Fiber | Infusion | Curing | Result |
|----|--|---|---|---|--|--|
| 7 | Test resin reduction with vacuum instead of heat and test the removal of sizing. | 150g of resin reduced to 15.4 wt% IPA after 1:05hrs under vacuum. | Sizing Removed – Four ply's woven silica boiled to remove sizing. As-received – Four woven ply's stacked. | Heated resin to 80°C and infused at room temperature. | Heating pad with vacuum at 150°C for 3.5 hrs. and then in the oven at 225°C for 2 hours. | The resin reduced with a vacuum was in much better condition and flowed better. The final panels were in good condition. |
| 12 | Create a 2.5D panel thick enough to cut ablative samples from. | 347.8g of resin reduced to 15 wt% IPA after 1hrs under vacuum. | 12 ply's of woven silica sandwiched between 2 non-woven ply's and needle-punched. | Heated resin to 67°C and infused at room temperature. | After removing from the mold, the panel was hung in the oven and cured at 150°C and 225°C for 2 hours. | Good resin reduction, flow, and curing. 13.3mm thick panel with a 1.12 g/cc and 48.53 wt% resin content. |
| 14 | Create a 2.5D panel with more ply's. | - | 17 woven silica ply's sandwiched between 2 non-woven ply's | - | - | Too much distance between the non-woven ply's. Didn't fully join the preform in the z-direction. |
| 15 | Create a 2.5D panel with 3 non-woven ply's. | 403.10g of resin reduced to 18 wt% IPA | 1 non-woven 8 woven 1 non-woven 8 woven 1 non-woven | Room temperature VARTM. | Curing in compression press for 1.5 hrs. at 80°C (5 tons) for 150°C for 2 hours (1 ton). | Resin only wet out 80% of the panel. Need to redo the VARTM setup. |

Table 9 continued. Ablative panel experiments.

| | | | | | | |
|----|--|--|---|---|--|---|
| 16 | Create a 2.5D panel using the same preform as 15 but a heated VARTM setup. | 451.99g of resin reduced to 21.8 wt% IPA | 1 non-woven 8 woven 1 non-woven 8 woven 1 non-woven | 40°C VARTM with the resin heated to 66°C. | 2 hours in the compression press at 150°C and 1 ton of pressure with a final cure in the oven for 2 hours at 225°C. | Great resulting panel with an average density of 1.17 g/cc. |
| 17 | Create a 2.5D panel with a higher density. | 420.86g of resin reduced to 23.8 wt% IPA | 1 non-woven 9 woven 1 non-woven 9 woven 1 non-woven | 40°C VARTM with the resin heated to 66°C. | .5 hrs. in the compression press at 100°C, 1.5hrs at 150°C, 2hrs at 225°C at 1 ton, and 2 hours for the final cure in the oven for at 225°C. | Great resulting panel with a density between 1.35 and 1.82 g/cc. |
| 19 | Produce two more 2.5D ablative panels | - | - | - | - | Experiment stopped due to needle-punching issues. |
| 20 | Create 2.5D ablative panel with new needle-punching parameters. | 470g of resin reduced to 26 wt% IPA | 1 non-woven 8 woven 1 non-woven 8 woven 1 non-woven | 40°C VARTM with the resin heated to 66°C. | .5 hrs. in the compression press at 100°C, 1.5hrs at 150°C, 2hrs at 225°C at 1 ton, and 2 hours for the final cure in the oven for at 225°C. | High quality panel produced with an average density of 1.28 g/cc. |

Table 9 continued. Ablative panel experiments.

| | | | | | | |
|----|---|--|---|---|--|--|
| 22 | Produce 2D and 2.5D ablative samples with the same resin reduction. | 659.89g of resin reduced to 26.9 wt% IPA | 1 non-woven 8 woven 1 non-woven 8 woven 1 non-woven | 40°C VARTM with the resin heated to 66°C. | .5 hrs. in the compression press at 100°C, 1.5hrs at 150°C, 2hrs at 225°C at 1 ton, and 2 hours for the final cure in the oven for at 225°C. | High quality 2D and 2.5D panels of the same thickness with densities within 0.05 g/cc. |
| 24 | Produce a 2.5D panel with 20 minutes of needle-punching. | 793.12g of resin reduced to 19.5 wt% IPA | 1 non-woven 8 woven 1 non-woven 8 woven 1 non-woven | 40°C VARTM with the resin heated to 64°C. | .5 hrs. in the compression press at 100°C, 1.5hrs at 150°C, 2hrs at 225°C at 1 ton, and 2 hours for the final cure in the oven for at 225°C. | High quality 2.5D ablative panel with 20 minutes of needle-punching. |
| 25 | Produce a 2.5D panel with 40 minutes of needle-punching. | Resin shared with experiment 24. | 1 non-woven 8 woven 1 non-woven 8 woven 1 non-woven | 40°C VARTM with the resin heated to 64°C. | .5 hrs. in the compression press at 100°C, 1.5hrs at 150°C, 2hrs at 225°C at 1 ton, and 2 hours for the final cure in the oven for at 225°C. | High quality 2.5D ablative panel with 40 minutes of needle-punching. |

Table 10. Mechanical testing panel experiments.

| | Purpose | Resin | Fiber | Infusion | Curing | Result |
|----|--|--|-------------------------------------|---|---|---|
| 18 | Produce 2D and 2.5D ILSS samples for testing | 100g of resin reduced to 24 wt% IPA | 1 non-woven 3 woven 1 non-woven | 40°C VARTM with the resin heated to 66°C. | 0.5 hrs. in the compression press at 100°C, 1.5hrs at 150°C, 2hrs at 225°C at 1 ton, and 2 hours for the final cure in the oven for at 225°C. | Good panels with the same thickness for ILSS testing. |
| 21 | Produce 2D and 2.5D flexural test samples. | 680.43g of resin reduced to 24.8 wt% IPA | 1 non-woven 3 woven 1 non-woven | 40°C VARTM with the resin heated to 66°C. | 0.5 hrs. in the compression press at 100°C, 1.5hrs at 150°C, 2hrs at 225°C at 1 ton, and 2 hours for the final cure in the oven for at 225°C. | High quality test panels of uniform and comparable thicknesses. |
| 26 | Produce 2D and 2.5D panels large enough to cut tensile and compression samples from. | 1,450.4g of resin reduced to 26 wt% IPA | 1 non-woven 3 woven 1 non-woven | 40°C VARTM with the resin heated to 66°C. | 0.5 hrs. in the compression press at 100°C, 1hrs at 150°C, and 2 hours for the final cure in the oven for at 225°C. | The infusion went well and the panels looked good going into the oven for curing. During curing, the panels warped badly and were unusable. |
| 27 | Produce 2D and 2.5D panels large enough to cut tensile and compression samples from. | 1526.48g of resin reduced to 24 wt% IPA | 1 non-woven 3 woven 1 non-woven | 40°C VARTM with the resin heated to 66°C. | 0.5 hrs. in the compression press at 100°C, 1hrs at 150°C, and 2 hours for the final cure in the compression press at 225°C. | The infusion and cure went well producing usable test panels. |

III. PERFORMANCE EVALUATION

Mechanical Testing

Flexural and interlaminar shear strength were measured to compare the mechanical properties between the 2D and needle-punched composites. Flexural samples were prepared with three woven silica plies sandwiched between two non-woven mat silica plies. Five 2D flexural samples were tested, averaging 7.3 mm in thickness and 13.1 mm in width. Span for the beam test was set at a 16:1 ratio following ASTM D7264 standards at 117.1 mm. Six needle-punched samples averaging 6.8 mm thickness and 13.1 mm width were tested with a support span for the 3-point bending test set at 109.5 mm.

Interlaminar shear strength was determined using a short-beam 3-point bending test following ASTM D2344 standards. Six 2D and needle-punched samples were processed using a similar construction to the flexural samples, three woven silica plies sandwiched between two non-woven mat silica plies. The 2D and needle-punched samples had an average thickness of 6.2 mm and a width of 12.4 mm, and the support span was set at 37 mm, a 6:1 ratio of the thickness. Testing was conducted on an MTS 810 Material Testing System.

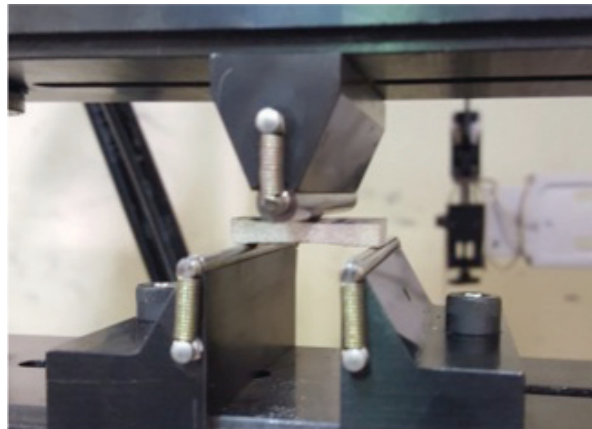


Figure 15. Short beam testing.

Microstructural analysis of the 2D and needle-punched samples was conducted to observe the effects of needle-punching on the woven and non-woven layers. An FEI Helios NanoLab 400 SEM was used, and samples were sputter coated with Iridium to enhance conductivity. Cross-sections were exposed using waterjet cutting.

Twelve by thirteen inch 2D and 2.5D panels were created using a similar structure as the flexural and short beam panels in order to perform tension testing of the material. Based on ASTM D3039 standards, 1" x 10" samples were cut for tensile testing. Testing was conducted on an MTS 810 Material Testing System according to ASTM standards.

Thermal Properties Testing

TGA Experiment. A Shimadzu TGA-50 thermogravimetric analyzer was used to measure the weight of woven and non-woven samples from the 2.5D composite to measure the changes in mass loss as the temperature increased. A woven sample from the 2D formulation was measured as well to compare and contrast the effect of needle-punching on mass-loss. Samples were tested in N₂ and air utilizing a procedure defined by NASA, first heating the sample to 150°C and holding it there for 30 minutes to dry the sample. Then the sample was heated at 20°C/minute to 1,000°C [19].

Ablation Testing. Oxyacetylene test bed (OTB) testing was conducted on each 2D and 2.5D formulation. The OTB setup shown in Figure 16 and 17 simulates the harsh environment endured by an ablative composite. Each sample was tested at a 1,000 W/cm² heat flux for 40 seconds. An example of a similar material test is shown in Figure 18. The OTB continuously collects data via a thermocouple embedded 10 mm from the backside of the ablative plug to measure backside heat-soaked temperatures. A LumaSense Technologies ISQ5 two-color IR pyrometer and an M9104 Mikron IR video

camera are used to measure surface temperature across the ablative surface throughout the test, and a DALSA DS-21-04m12-12e HD video camera captures changes on the surface throughout the trial. These data allow for the collection of mass loss, char yield, recession rate, heat-soaked temperature, and surface temperature.

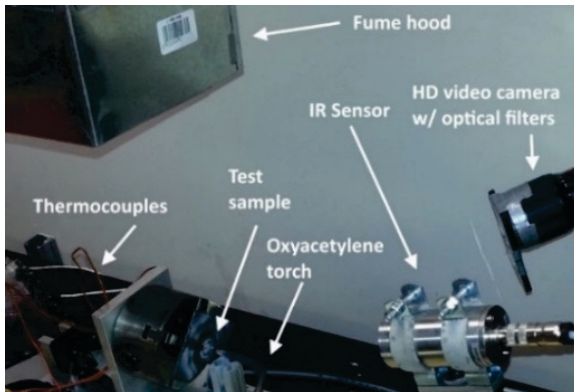


Figure 16. Oxyacetylene test bed at UT Austin [9].

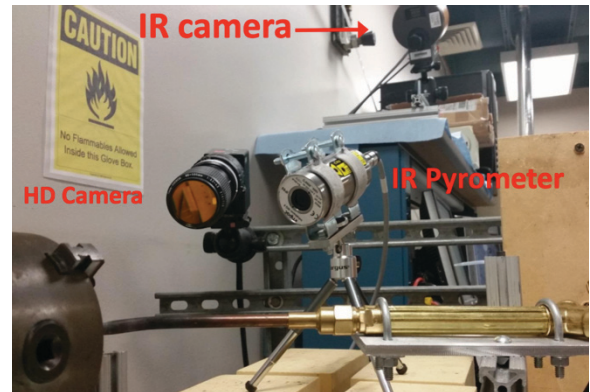


Figure 17. Instrumentation on an oxyacetylene test bed at UT Austin [20].



Figure 18. Sample being tested on the oxyacetylene test bed.

To achieve a $1,000 \text{ W/cm}^2$ heat flux, a neutral 1.1:1 fuel ratio was set up for the oxyacetylene torch. This neutral flame helps to reduce oxidation of the ablative material. Calibration was done with a #4 victor welding tip and a Vatell Gardon heat flux transducer (Thermogage 1000-54) [21]. For preliminary testing, at least three ablative samples were created from each formulation with an 18-19 mm diameter and a thickness of 14-16 mm. Representative samples are shown in Figure 19. Holes were drilled in the backside of each sample to accommodate a miniature (0.55 mm diameter) type-K thermocouple placed 10 mm from the sample side exposed to the flame.



Figure 19. Needle-punched ablation samples.

IV. RESULTS AND DISCUSSION

Mechanical Properties Testing

Interlaminar Shear Strength. Interlaminar shear stress results are shown in Figures 11. Figure 11b shows the needle-punched composite presented a 27% higher interlaminar shear strength over the standard 2D laminate composite. Table 11 contains a summary of the mechanical properties observed, including coefficient of variance calculations.

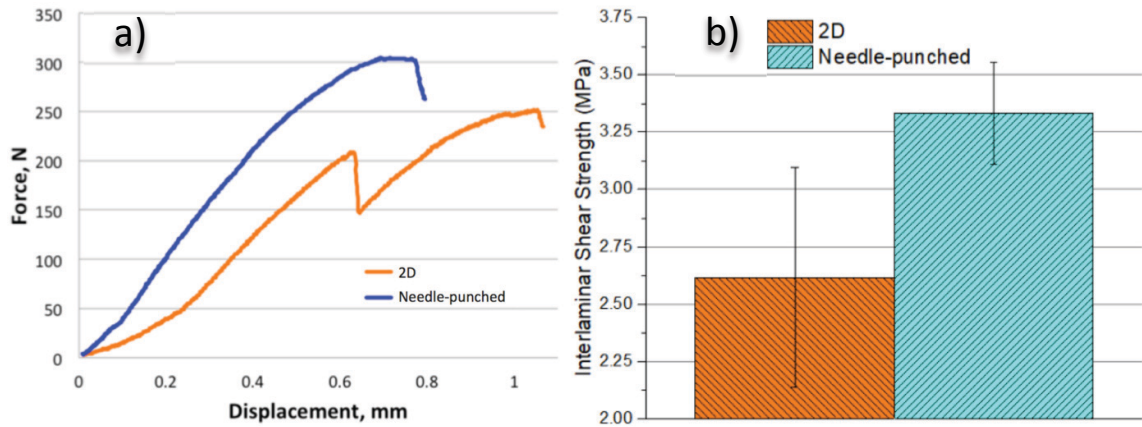


Figure 20. (a) Representative interlaminar shear and (b) cumulative interlaminar shear test results.

Table 11. ILSS properties summary.

| | ILSS (Mpa) | COV (%) |
|------|---------------|------------|
| 2D | 2.62 ± 0.48 | 18.3% |
| 2.5D | 3.33 ± 0.22 | 6.68% |

Flexural Test. Flexural results are shown in Figures 21 through 22. The needle-punched composite presented an impressive 181% improvement in flexural strength over the standard 2D laminate composite as shown in Figure 22a. The flexural modulus between the two composites was similar, with a slight increase of 2% in the flexural modulus observed in the needle-punched composites as shown in Figure 22b. Table 12

contains a summary of the mechanical properties observed, including coefficient of variance calculations.

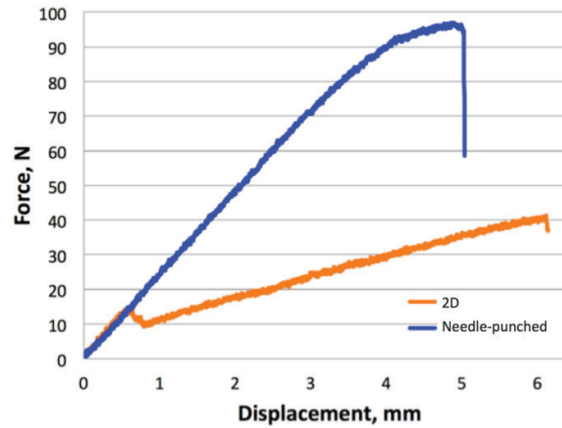


Figure 21. Representative flexural test results.

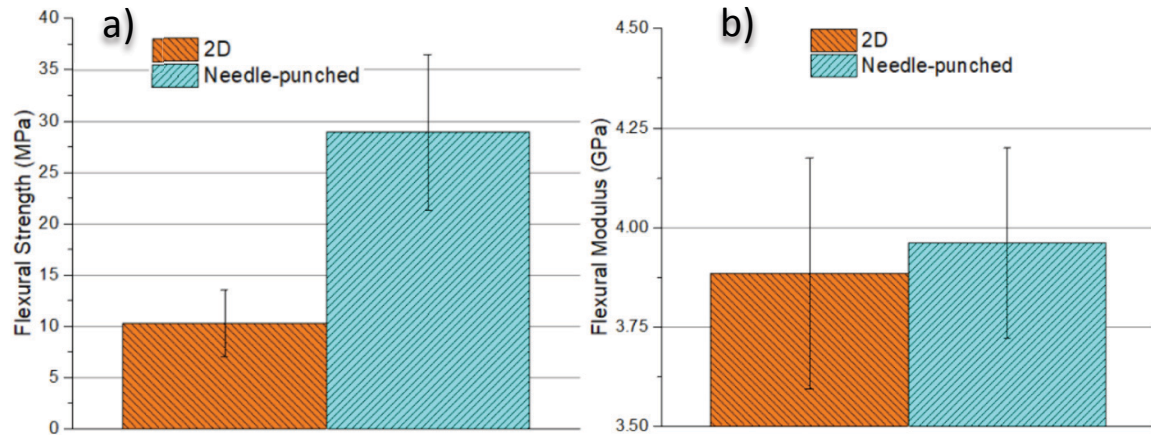


Figure 22. Flexural (a) strength and (b) modulus results.

Table 12. Flexural properties summary.

| | Flexural Strength (Mpa) | COV (%) | Flexural Modulus (Gpa) | COV (%) |
|-------------|----------------------------|------------|---------------------------|------------|
| 2D | 10.26 ± 3.27 | 31.89% | 3.89 ± 0.29 | 7.49% |
| 2.5D | 28.89 ± 7.58 | 26.24% | 3.96 ± 0.24 | 6.03% |

Tension Properties Testing. Tensile properties testing results are shown in Figure 23. The tensile strength for the 2D and 2.5D samples had a much lower coefficient of variance than the flexural and interlaminar shear stress samples. The needle-punching process, if done in excess runs the risk of damaging the woven fibers

reducing in-plane strength. The test results for the 2D and 2.5D ultimate tensile strength was within 2.58%, with the 2.5D samples slightly outperforming 2D. The tensile modulus results exhibited a much higher standard coefficient of variance in excess of 60% as detailed in Table 13; however, the modulus for the 2D and 2.5D were within 3.86% of each other. Overall, the 2.5D performed on par with the 2D formulation with no detriment to its tensile strength.

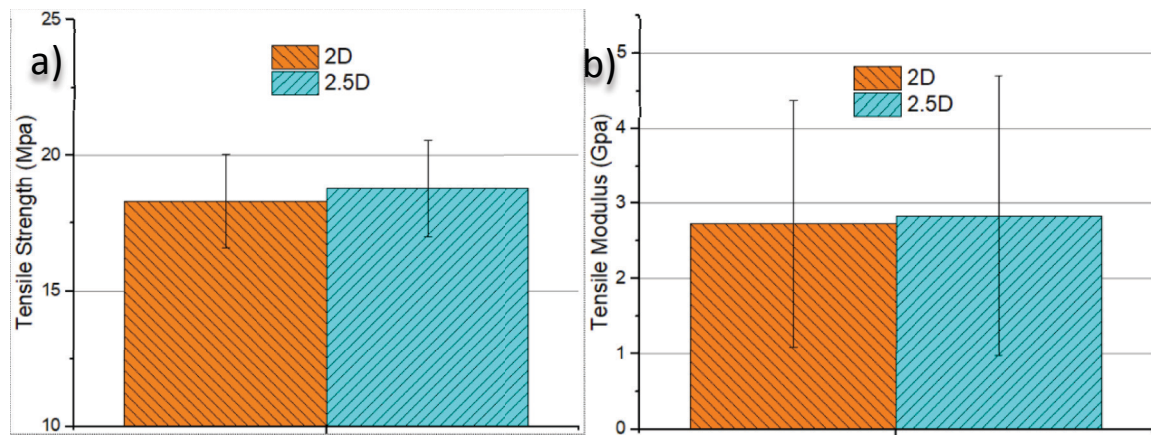


Figure 23. Tensile (a) strength and (b) modulus results.

Table 13. Tensile properties summary.

| | Tensile Strength (Mpa) | COV (%) | Tensile Modulus (Gpa) | COV (%) |
|------|---------------------------|------------|--------------------------|------------|
| 2D | 18.31 ± 1.72 | 9.41% | 2.73 ± 1.64 | 60.03% |
| 2.5D | 18.78 ± 1.78 | 9.52% | 2.84 ± 1.86 | 65.58% |

Thermal Properties Testing

TGA Results. Schellhase et al. performed thermogravimetric analysis on the Techneglas UHTR neat resin system to compare it with SC-1008, a phenolic resin commonly used in thermal protection systems. The results, shown in Figure 24a provide insight into the high char yield produced by UHTR when compared to phenolic resin [9]. The results for phenolic resin agree with those produced by Boghozian et al. in Figure 3. The derivative of the TGA measurements shown in Figure 24b highlight chemical

reactions occurring at different temperatures for both neat resin systems. SC-1008 has three peaks, at 410°C, 511°C, and 655°C while UHTR only has two peaks, each smaller than those for SC-1008 and at higher heating rates (722°C and 873°C) [9].

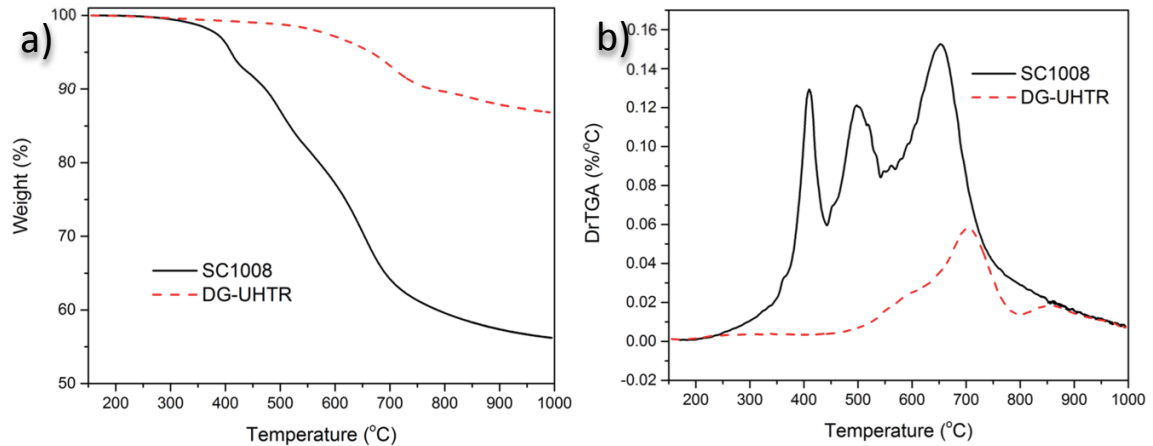


Figure 24. (a) TGA and (b) DrTGA for neat resin systems [9].

To understand the influence of the fiber reinforcement on the performance of the final composite at high heat fluxes a thermogravimetric analysis was conducted on the woven and non-woven sections of the 2.5D composite, each completed in N₂ and air. To understand the effect needle-punching has, a woven sample was tested from the 2D composite as well. In Figure 25a, while all composites performed very well, the 2D woven section had the lowest mass-loss. The non-woven section of the hybrid composite contained a higher resin content, which explains the higher mass-loss visible in the TGA chart. Derivatives of each TGA were taken to understand chemical reactions taking place across the heating range. Similar to the neat resin system results, the Techneglas-based composite showed two reaction points, however, they occurred at lower temperatures – 555°C and 763°C. As shown in Figures 25b and 27b, the same samples were analyzed in air. For the non-woven 2.5D, woven 2.5D, and woven 2D a higher mass-loss occurred. The peak changes in the derivative of the TGA were nearly double at each inflection

point, explaining the greater mass-loss over time. The TGA studies are conducted in air to observe how the material will perform in a natural atmospheric environment. Any organic compounds will react in the air environment leading to the higher mass loss.

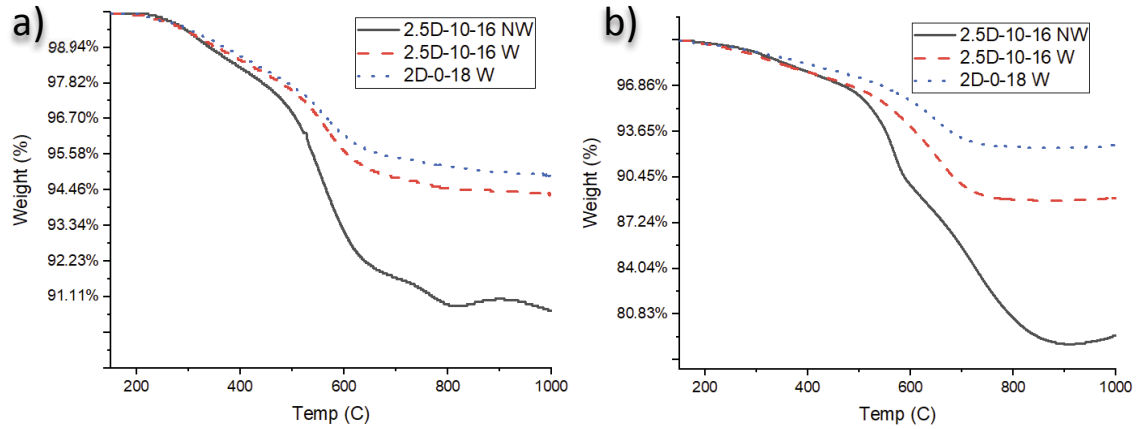


Figure 25. (a) TGA in N₂ and (b) TGA in air.

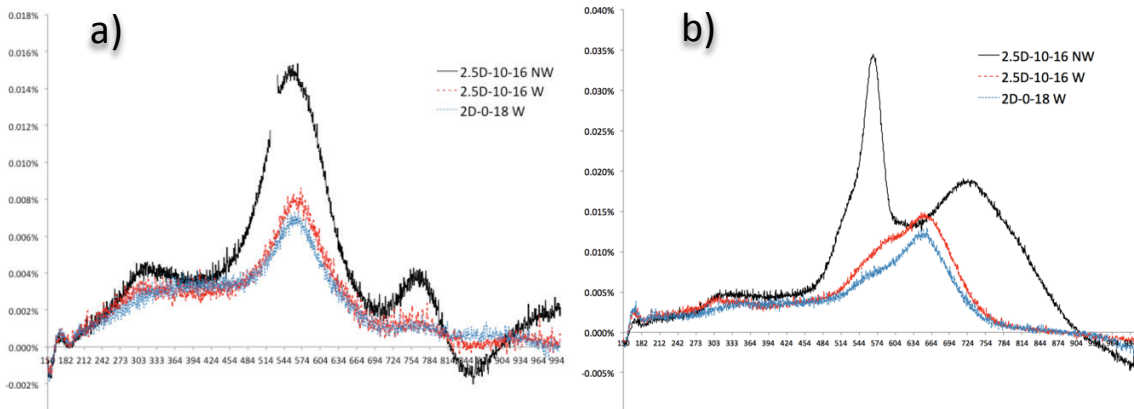


Figure 26. (a) DrTGA in N₂ and (b) DrTGA in air.

OTB Results. Five ablation panels outlined in Table 14 were created in addition to the MX-2600 tested by Schellhase et al. The 2D and 2.5D formulations were used to examine the influence of architecture, density, and needle-punching on the composites ability to resist the harsh 1,000 W/cm² heat flux for 40 seconds.

Table 14. Summary of test composites [9].

| Composite | Architecture | Non-woven Plies | Woven Plies | Needle-punching (mins) |
|--------------|------------------|-----------------|-------------|------------------------|
| MX-2600 | Molding Compound | n/a | None | 0 |
| 2D-0-18 | 2D | 18 | 3 | 0 |
| 2.5D-10-16 | 2.5D | 16 | 3 | 10 |
| 2.5D-10-18F1 | 2.5D | 18 | 3 | 10 |
| 2.5D-20-18 | 2.5D | 18 | 3 | 20 |
| 2.5D-40-18 | 2.5D | 18 | 3 | 40 |

Molding Compound, 2D, and 2.5D Comparison. Density's varied across the three panels from 1.13 g/cc to 1.71 g/cc as shown in Figure 27a. The 2D and 2.5D densities were lower than the MX-2600 tested by Schellhase et al. The lower density is attributed to the different processing method, Schellhase et al. used a custom mold with high pressure in a compression press, whereas, the two sample panels in this study were produced with a vacuum assisted resin transfer molding process. Variation in the density across the 2D and 2.5D sample panels has to do with the number of silica plies and the processing parameters. Sample 2.5D-10-16 had the lowest density, 1.13 g/cc, this was accomplished by manufacturing the composite with two less woven silica plies in a composite of the same thickness. The resin content by weight percent is shown in Figure 27b, which illustrates the amount of resin contained in each composite panel.

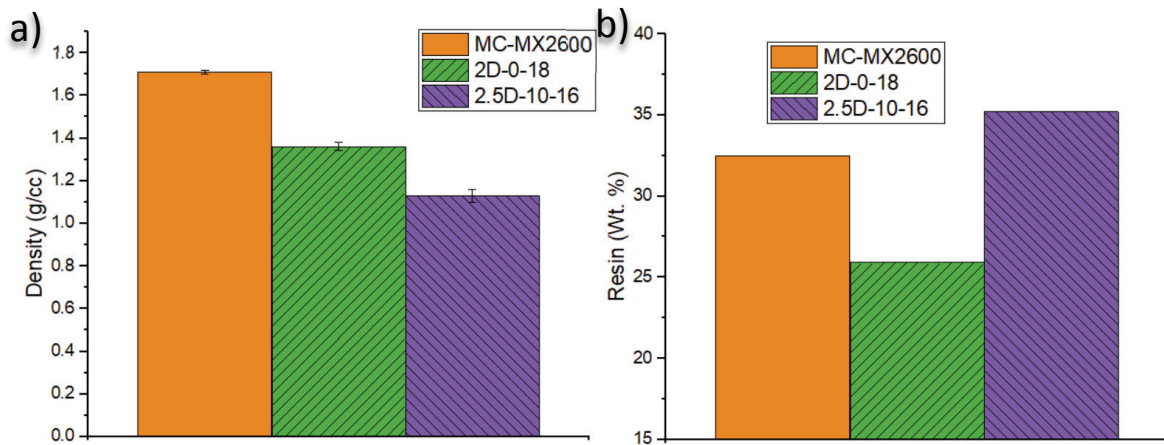


Figure 27. (a) Density and (b) wt% resin in composites [9].

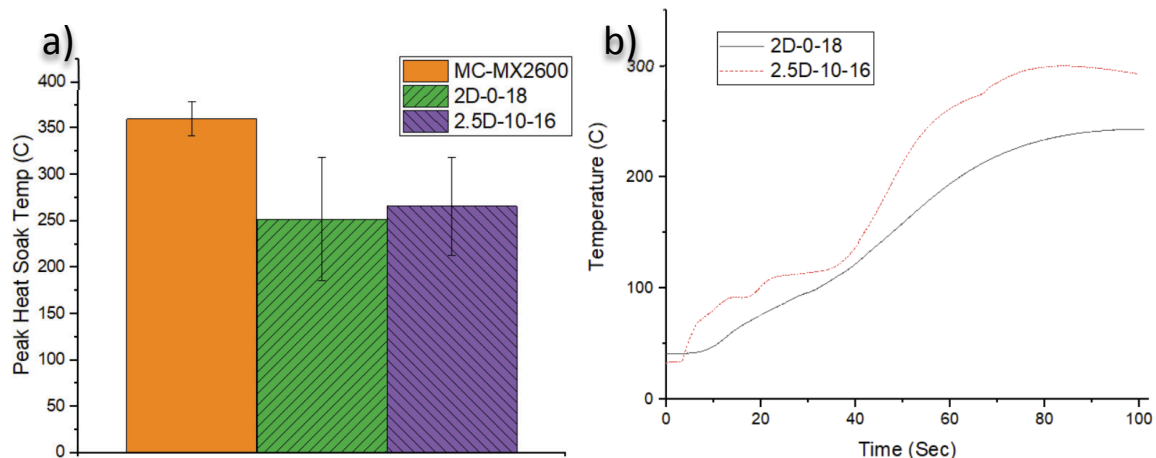


Figure 28. (a) Peak heat-soaked temperature and (b) backside temperature over time for 2D and 2.5D ablatives [9].

The thickness of each sample was measured before and after each test to determine the overall recession. Post-test samples were measured with a dial gauge because cratering was often present after ablation as shown in Figure 29. Recession rates were calculated as a measure of millimeters per second (mm/s) by averaging the recession across the total 40-second exposure time. Lower recession rates are indicative of a material's ability to withstand the high heat flux without significant material degradation. At the high heat flux and long exposure time, as the heat traveled through the thickness, the 2D and 2.5D formulations were susceptible to delamination causing higher standard deviations in the data. The 2D-0-18 formulation experienced a 0.100 mm/s recession rate, while the 2.5D formulation, 2.5D-10-16 had a recession rate of 0.070 mm/s and the MX-2600 molding compound tested by Schellhase et al. had a recession rate of 0.058 mm/s.

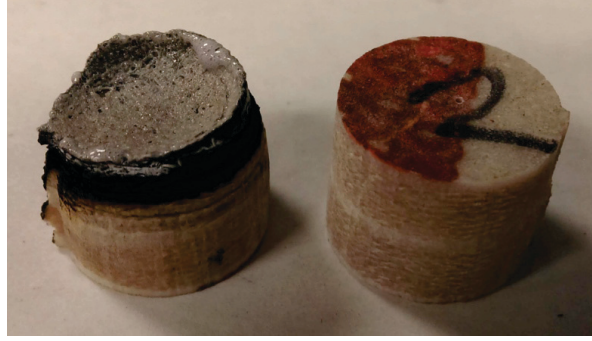


Figure 29. Post-test sample (left) and pre-test sample (right).

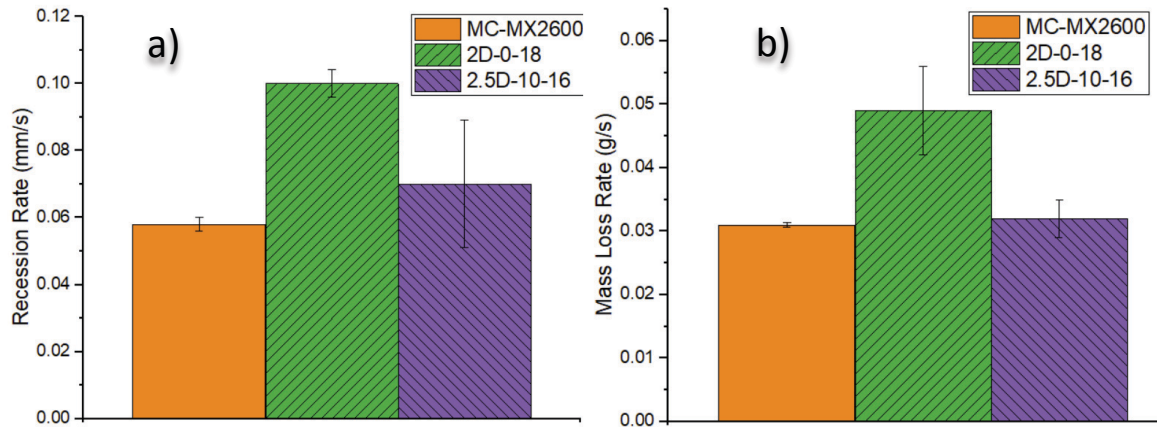


Figure 30. (a) Recession rate (mm/s) and (b) mass loss rate (g/s) of different ablatives [9].

Mass loss (%), char yield (%), and mass loss rate were calculated by weighing the sample before and after each ablation test. The 2.5D formulation outperformed the 2D and MX-2600 formulations in two categories with 2.5D-10-16 producing the lowest mass loss percentage and subsequently the highest char yield as shown in Figure 31.

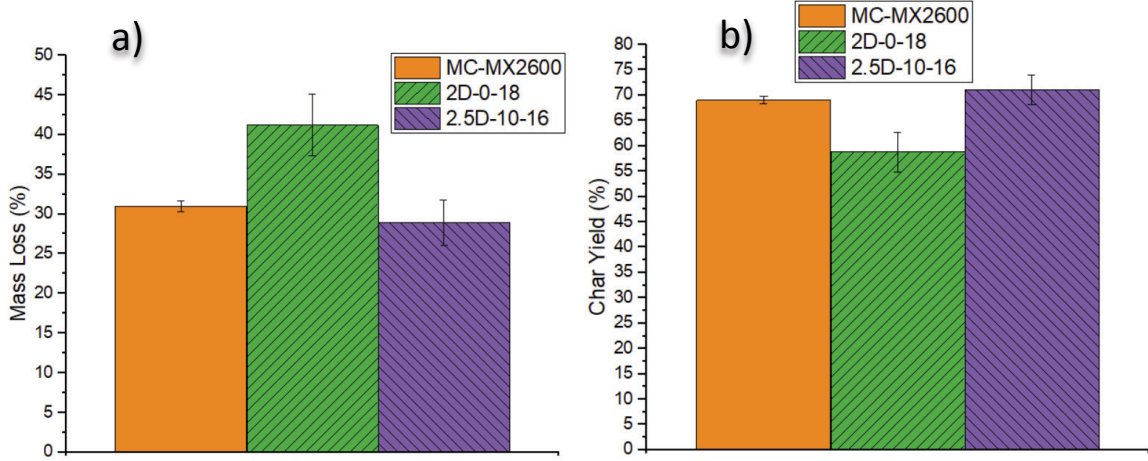


Figure 31. (a) Mass loss (%) and (b) char yield (%) of different ablative materials [9].

Table 15 catalog's the results of the ablation testing for the 2D and 2.5D formulations from this study and the molding compound composite produced by Schellhase et al. Overall, the 2.5D-10-16 composite produced in this study produced better PHST results and comparable recession rate, mass loss, and char yield to the SOTA MX-2600 formulation at a much lower density (1.13 g/cc versus 1.71 g/cc).

Table 15. Summary of collected OTB data for molding compound, 2D, and 2.5D [9].

| Architecture | Material | Density (g/cc) | Resin Content (wt%) | PHST (°C) | Recession Rate (mm/s) | Mass Loss (%) | Mass Loss Rate (g/s) |
|------------------|-------------|----------------|---------------------|--------------|-----------------------|---------------|----------------------|
| Molding Compound | S/Ph MX2600 | 1.71 ± 0.01 | 30-35 | 360.0 ± 18.0 | 0.058 ± 0.002 | 31.0 ± 0.7 | 0.031 ± 0.0003 |
| 2D | 2D-0-18 | 1.36 ± 0.03 | 25.9 | 251.8 ± 66.2 | 0.100 ± 0.044 | 41.2 ± 3.86 | 0.049 ± 0.007 |
| 2.5D | 2.5D-10-16 | 1.13 ± 0.03 | 35.2 | 265.8 ± 52.9 | 0.070 ± 0.019 | 28.9 ± 2.88 | 0.032 ± 0.003 |

Surface temperatures for the 2D and 2.5D formulations were captured using an infrared two-color pyrometer over time and shown in Figure 32. The surface temperature for the 2.5D formulation rose more slowly and exhibits less variance. The 2D formulations were highly susceptible to delamination, which was captured in the high-definition (HD) video. In the first snapshot at 10 seconds, you can easily see a layer of the ablative peeled away from the surface and ready to fall. The 2D formulation is then unable to form a char layer to enhance the reduction of ablation recession. Snapshots

were captured at 10-second intervals of the HD and IR video to show the integrity of the material over time. It's important to note that the temperature scale for the molding compound in Figure 33 is different than the 2D and 2.5D samples because they were taken at different times. However, when comparing the 2D and 2.5D snapshots, the delamination of the 2D samples is evident, and the center of the 2.5D sample stays cooler throughout the 40 seconds. This is confirmed by the IR pyrometer measurements in Figure 32. To better understand the rate at which each ply either delaminated or visibly burned through, a study was conducted using the HD video to identify when ply's were burned through in Figure 34b. The rate at which the heat-flux penetrated the sample for the 2D was much faster, penetrating 6 plies within 40 seconds in contrast to 4 plies for the 2.5D formulation.

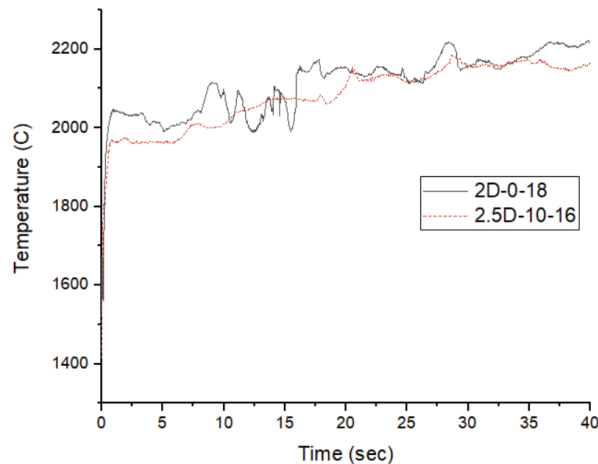


Figure 32. Surface temperature over time for 2D and 2.5D ablatives.

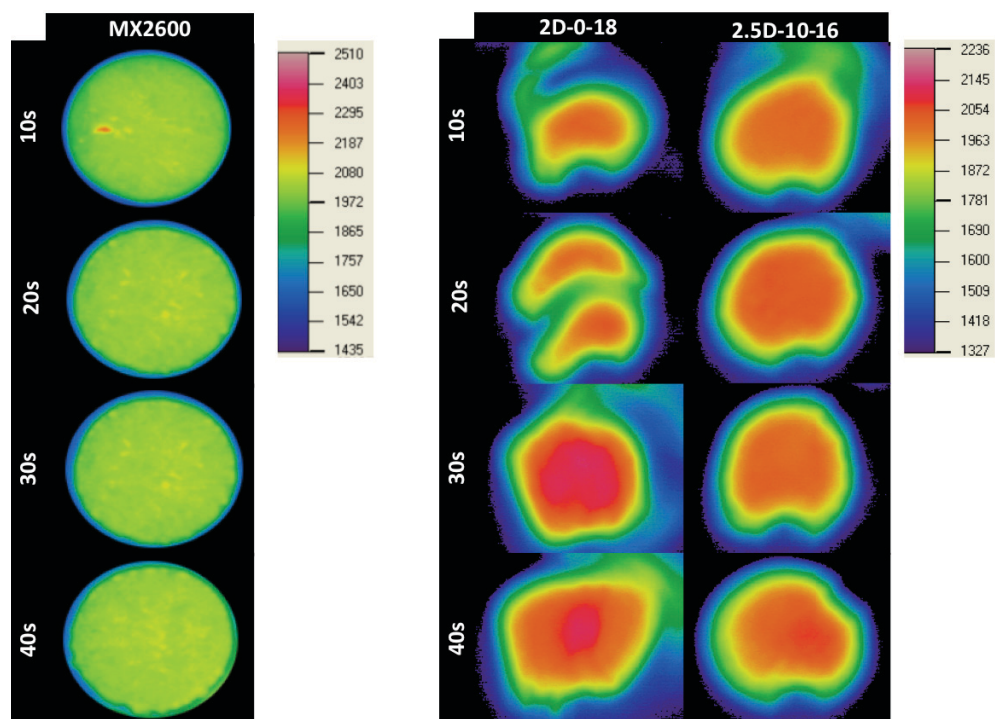


Figure 33. Infrared imagery of representative molding compound, 2D, and 2.5D samples [9].

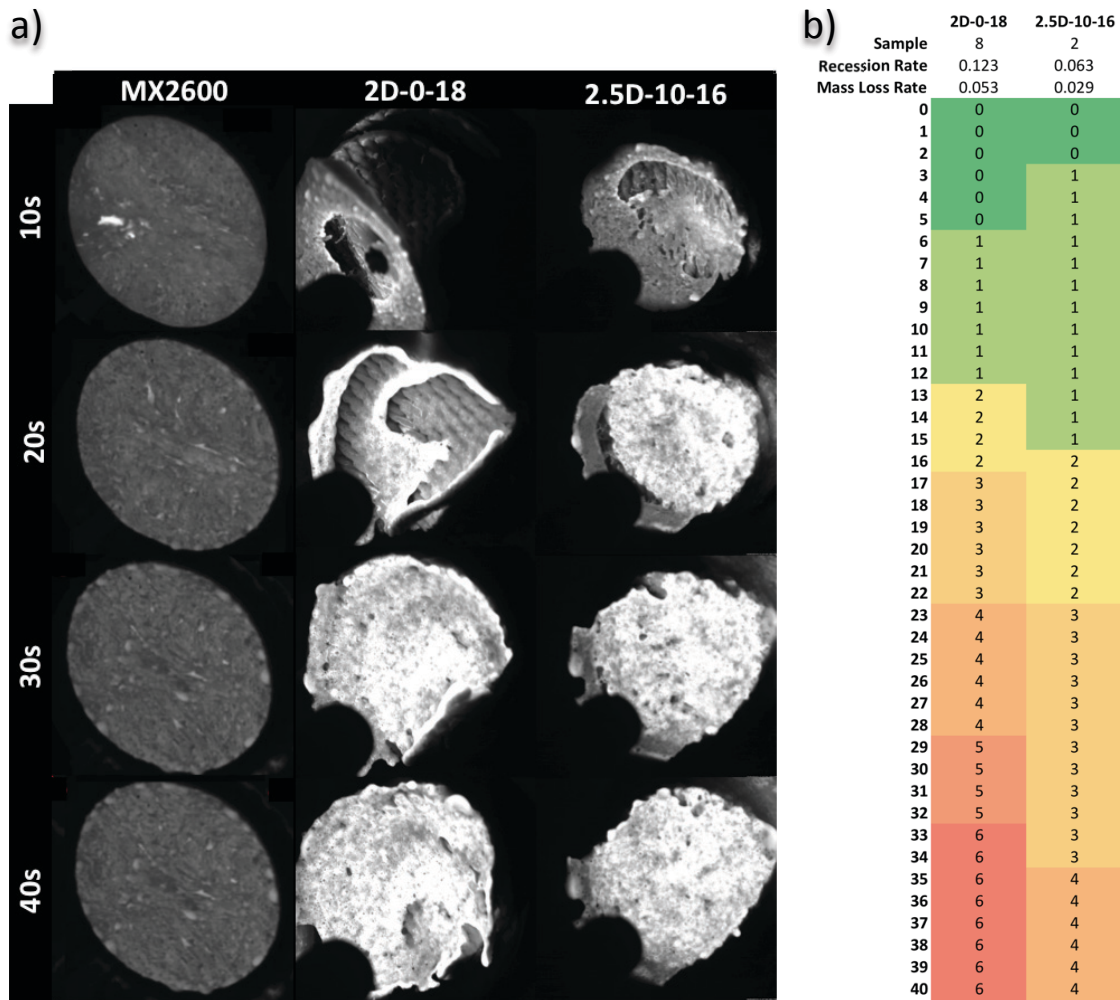


Figure 34. (a) High-definition imagery of representative molding compound, 2D, and 2.5D samples [9] and (b) ply burn-through over time for 2D and 2.5D representative samples.

Comparison of 2.5D Formulations with Increasing Needle-Punching. To

understand the relationship between needle-punching exposure and ablation performance, three panels were created as detailed in Table 14:

- 2.5D-10-18F1
- 2.5D-20-18
- 2.5D-40-18

Densities between the three panels were very close, as shown in Figure 35a; however, the amount of needle-punching time for each panel was 10 min, 20 min, and 40 minutes respectively. The resin content by weight percent is shown in Figure 35b, which illustrates the amount of resin contained in each composite panel.

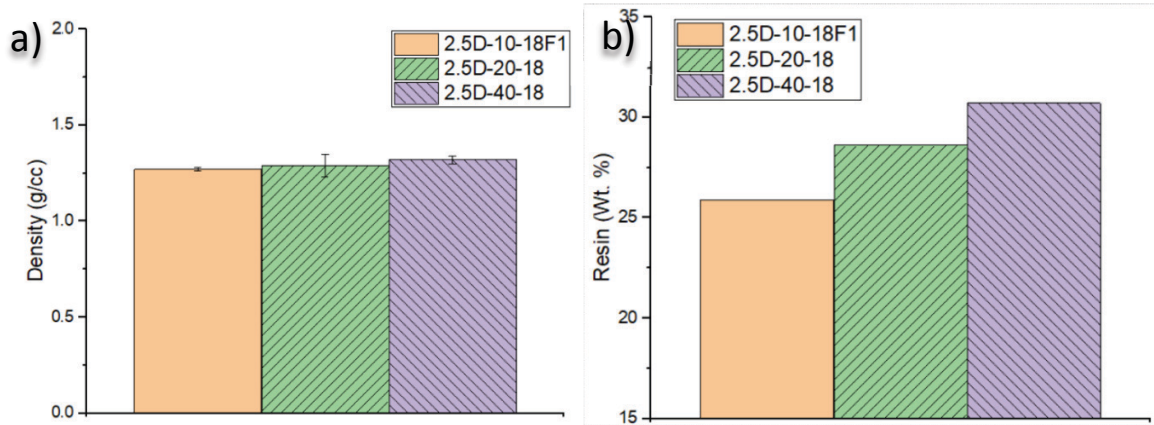


Figure 35. (a) Density and (b) wt% resin in 2.5D composites with increasing needle-punching time (10 min, 20 min, and 40 min).

The peak heat-soaked temperatures for the 2.5D samples ranged from 163.6°C to 204.2°C for the formulations as shown in Figure 36a, with 2.5D-40-18, the sample with 40 minutes of needle-punching recording the lowest heat-soaked temperature. An average backside temperature over time is shown in Figure 36b, with heat traveling much more slowly through the thickness in formulation 2.5D-40-18.

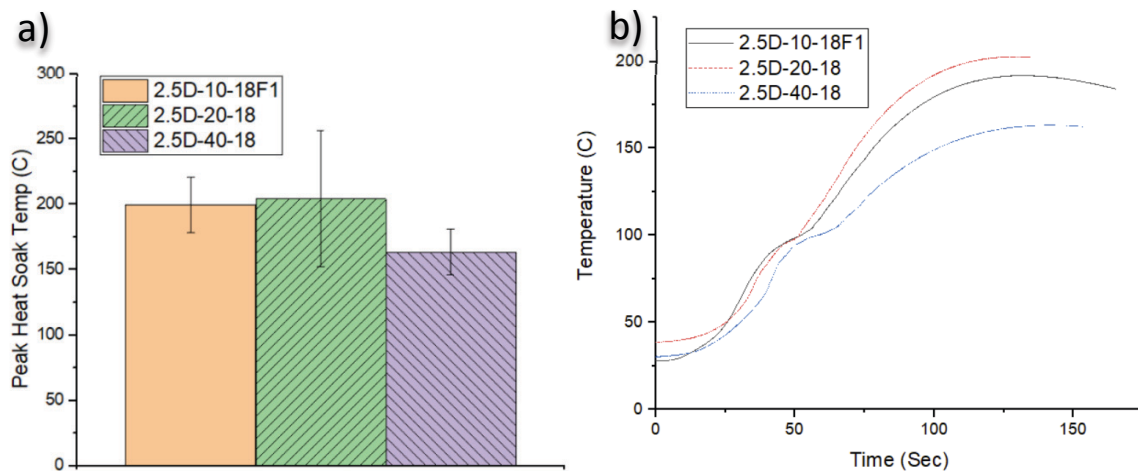


Figure 36. (a) Peak heat-soaked temperature and (b) backside temperature over time for 2.5D composites with increasing needle-punching time (10 min, 20 min, and 40 min).

The recession and mass-loss rates in Figures 37a and 37b show that changing the amount of needle-punching affects the final ablation resistance of the composite.

Increasing the needle-punching from 10 minutes to 20 minutes increased the performance by lowering the recession and mass-loss rates; however, when needle-punching was increased to 40 minutes the performance declined below that of the 10 minutes samples. Needle-punching has the ability to strengthen composites in the z-direction but it can have a detrimental effect on the fibers. With increased needle-punching, the likelihood of fiber breakage increases. The silica fibers are very brittle and as they are pushed through the thickness by the barbed needles they often break. With the increase of needle-punching to 40 minutes, the strength of the char layer reduced, and caused a faster recession and mass-loss rate.

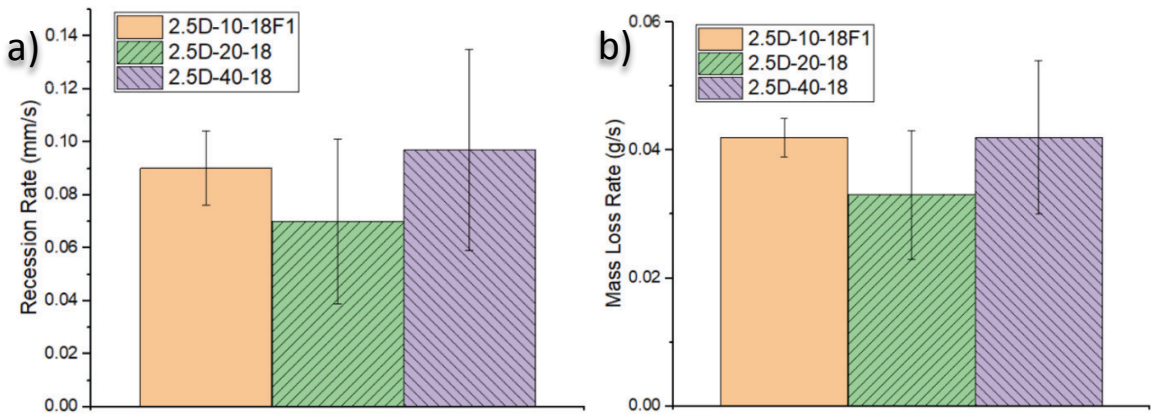


Figure 37. (a) Recession rate and (b) mass loss rate (g/s) in 2.5D composites with increasing needle-punching time (10 min, 20 min, and 40 min).

Mass loss (%) and char yield (%) were calculated by weighing the sample before and after each ablation test. Following the same trend as the recession rate, the formulation needle-punched for 20 minutes performed the best as shown in Figures 38a and 38b.

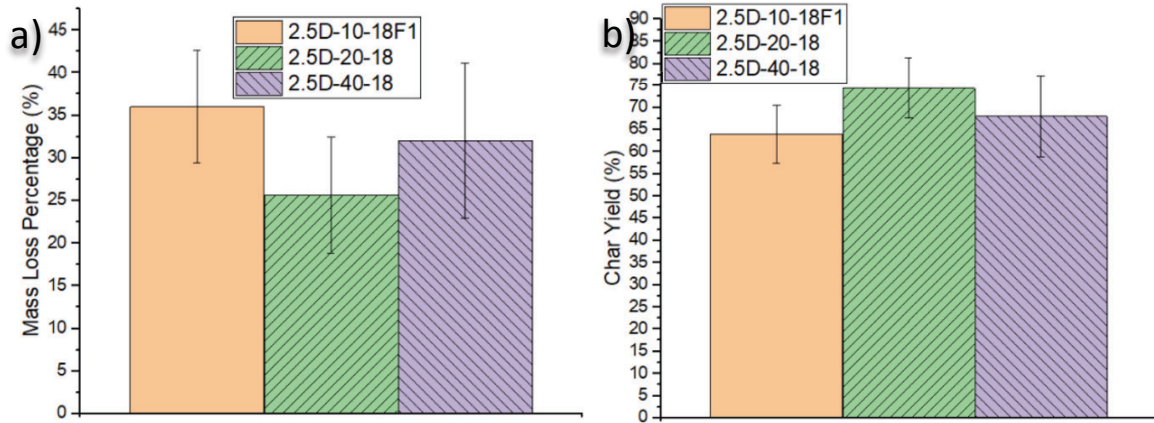


Figure 38. (a) Mass loss (%) and (b) char yield (%) in 2.5D composites with increasing needle-punching time (10 min, 20 min, and 40 min).

Table 16 summarizes the results of the needle-punching tests. Overall, the 2.5D-20-18 composite, with 20 minutes of needle-punching had the best recession rate, mass loss, and char yield.

Table 16. Summary of collected OTB data for 2.5D composites with increasing needle-punching time (10 min, 20 min, and 40 min).

| Architecture | Material | Density (g/cc) | Resin Content (wt%) | PHST (°C) | Recession Rate (mm/s) | Mass Loss (%) | Mass Loss Rate (g/s) |
|--------------|--------------|----------------|---------------------|--------------|-----------------------|---------------|----------------------|
| 2.5D | 2.5D-10-18F1 | 1.27 ± 0.01 | 25.9 | 199.5 ± 21.5 | 0.090 ± 0.014 | 36.0 ± 6.60 | 0.042 ± 0.003 |
| | 2.5D-20-18 | 1.29 ± 0.06 | 28.6 | 204.2 ± 52.1 | 0.070 ± 0.031 | 25.6 ± 6.79 | 0.033 ± 0.010 |
| | 2.5D-40-18 | 1.32 ± 0.02 | 30.7 | 163.6 ± 17.4 | 0.097 ± 0.038 | 32.0 ± 9.05 | 0.042 ± 0.012 |

Surface temperatures were captured over time for each formulation and average temperatures for each formulation are shown in Figure 39. Surface temperatures for each composite show variability, fluctuating from 2,000°C to 2,250°C. 2.5D-10-18F1 has the greatest variability due to the amount of delamination that occurred over time. By observing the infrared (IR) video and high-definition (HD) video delamination was visible as seen in Figures 40 and 41 where the ply's are visible curling as they melt and peel away from the surface of the sample. As expected based on the mass-loss and recession rate results, 2.5D-20-18 retained it's shape better throughout the 40 second ablation process with no visible delamination and consistent heat across the surface.

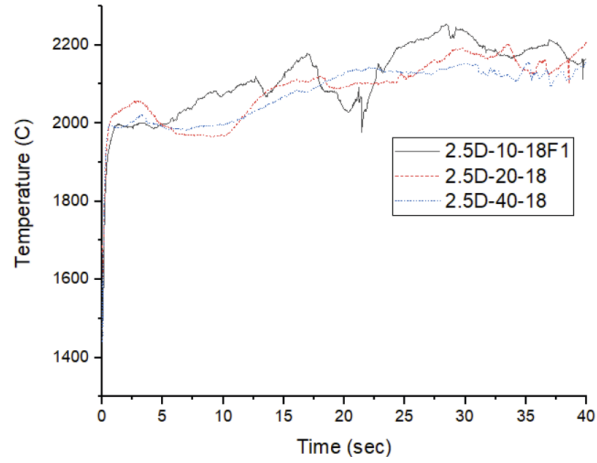


Figure 39. Surface temperature over time for 2.5D ablatives with increasing needle-punching time (10 min, 20 min, and 40 min).

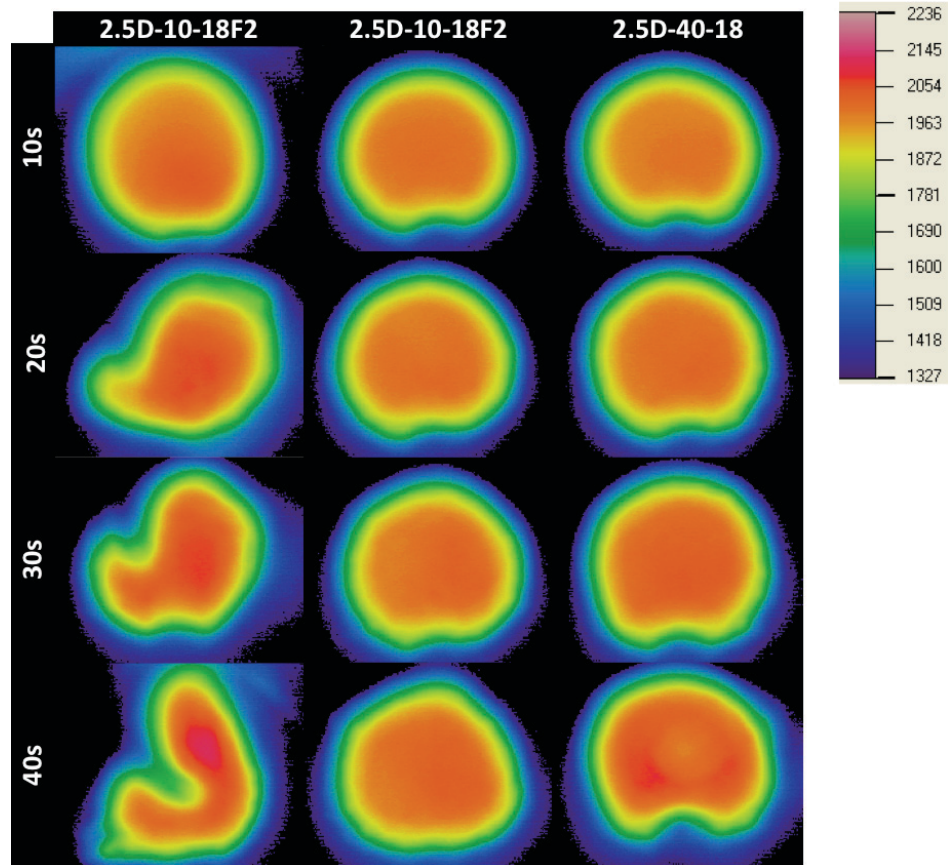


Figure 40. Infrared imagery of representative 2.5D samples with increasing needle-punching time (10 min, 20 min, and 40 min).

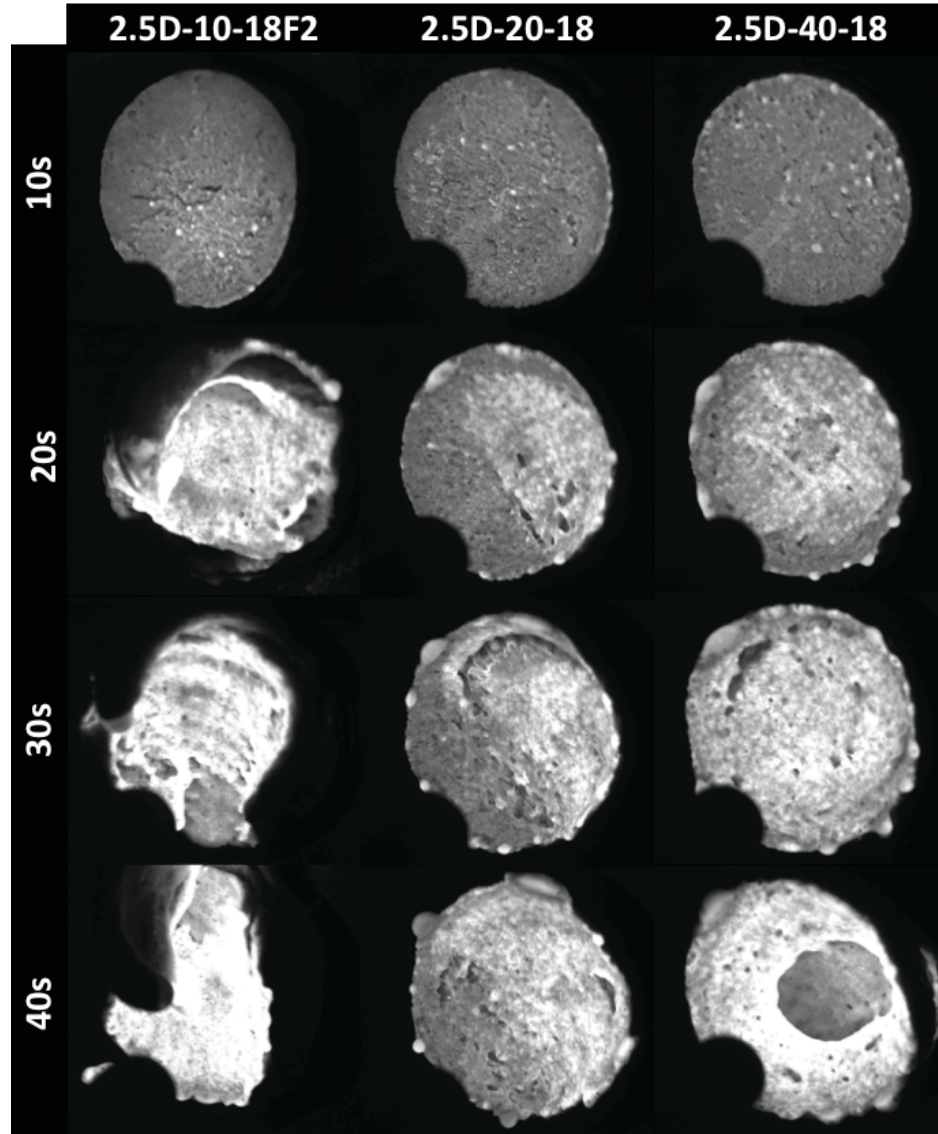


Figure 41. High-definition imagery of representative 2.5D samples with increasing needle-punching time (10 min, 20 min, and 40 min).

Microstructural Analysis using SEM

Interlaminar shear stress samples were cut and sputter coated to observe the change in fiber structure due to the needle-punching process. Figure 42a, shows the undisturbed silica fiber tows traversing the X-Y plane. Images at the woven/non-woven interface of the needle-punched composite are shown in figure 42b. The non-woven silica, being 100% silica contrasts well against the 96% woven silica. The non-woven fibers are drawn down into the woven plies with the barbed needle. Figure 42c shows

fiber breakage of the woven fibers as the needle traveled through the thickness. The random order of the fibers in the external non-woven ply is visible in Figure 42d.

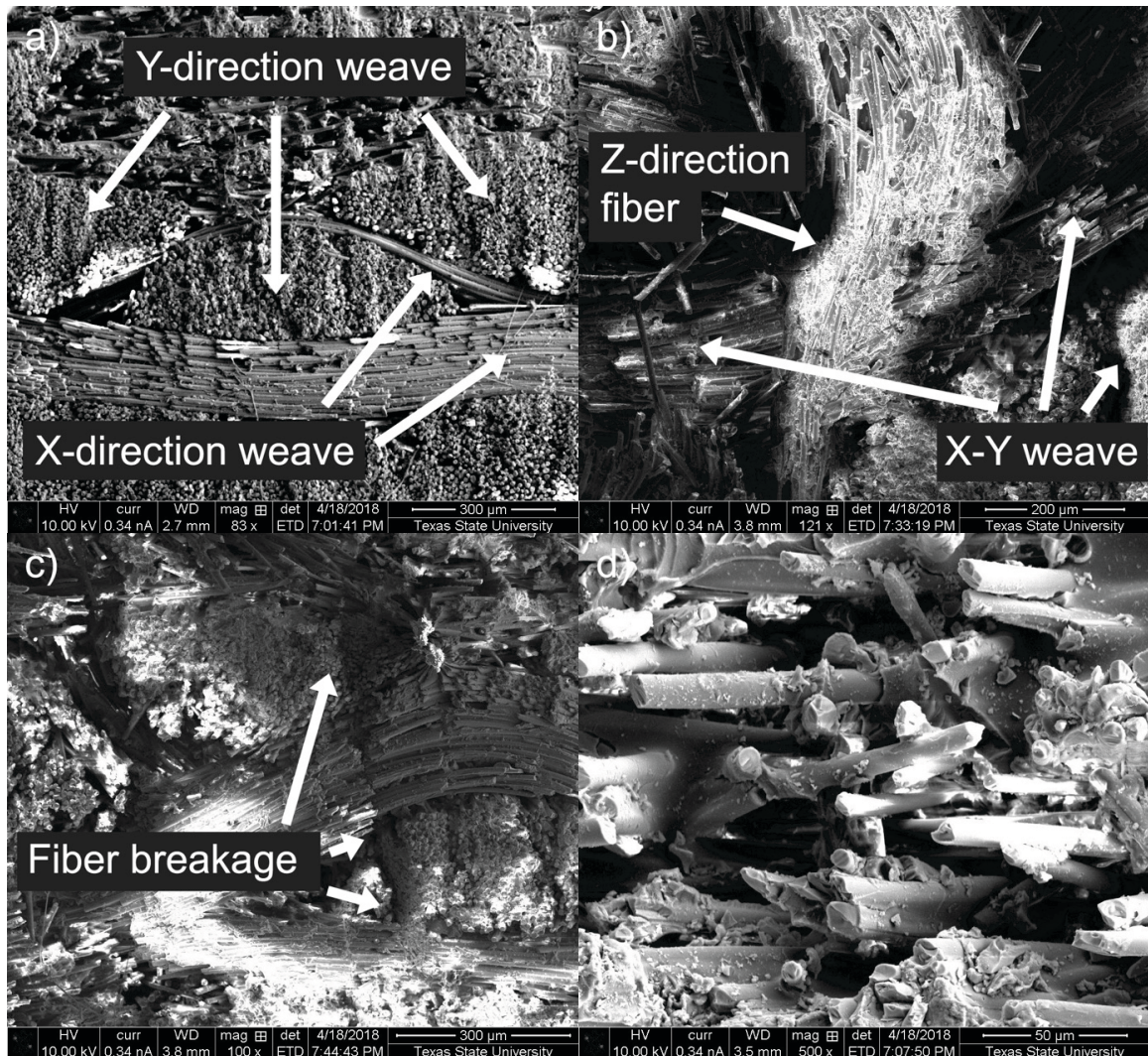


Figure 42. Scanning electron micrographs of 2D and 2.5D composites showing the (a) 2D composite cross-section, (b) 2.5D composite cross-section, (c) fiber breakage in the 2.5D composite, and (d) randomly ordered non-woven silica mat.

2.5D-10-16 samples were encased in epoxy to preserve the structure of the char layer after ablation testing and cross-section samples were cut. Cross-sections for the 2D composites were not preserved due to the char layer delaminating and separating during ablation. The 2.5D sample was then sputter coated with Iridium and observed under a scanning electron microscope at 50-500x to capture the char layer, heat affected zone

(HAZ), and virgin composite material as shown in Figure 43. The pyrolysis zone can be seen at the bottom of Figure 43b which is a 498x magnification of the char layer.

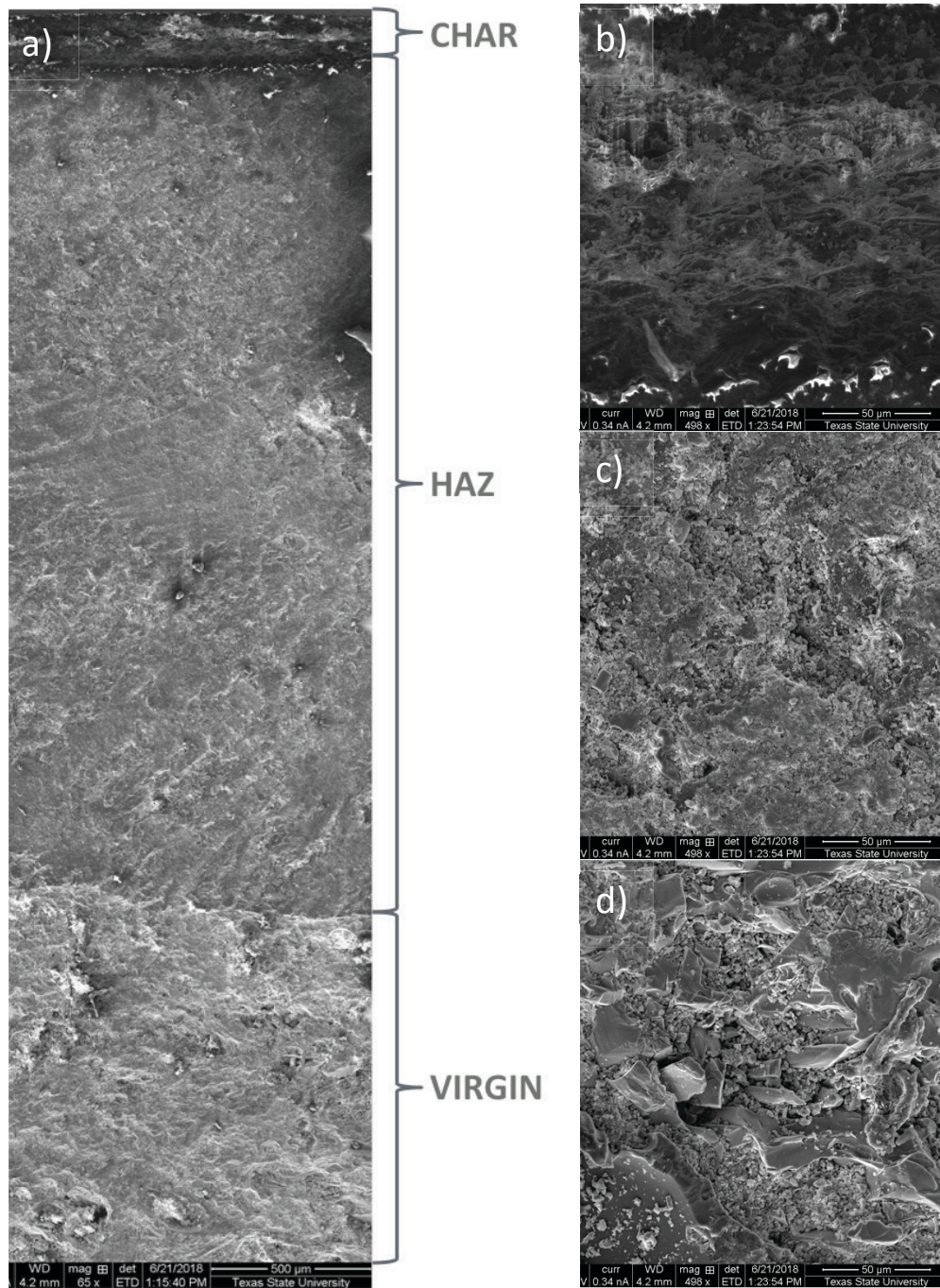


Figure 43. Scanning electron micrographs of 2.5D ablative composites showing the (a) entire cross-section, (b) char layer, (c) heat affected zone, and (d) virgin layer.

Analysis of Variance

Flexural, interlaminar shear, and tensile test results were compared using an analysis of variance (ANOVA) at a 95% confidence level (α 0.05) to determine the significance of the results. The statistics package, StatPlus:mac LE was used. The ability to compare the means from the 2D and 2.5D composites is identified by the p-value. The p-values for each mechanical result is identified in Table 17. A p-value of 0.05 or greater corresponds to means that are similar, while p-values less than 0.05 identify means that are significantly different. The p-value greater than 0.05 signifies that there are no significant differences between the flexural modulus, tensile strength, or tensile modulus means; however, the p-value for the flexural strength and interlaminar shear strength indicates that there may be a difference in the means and further testing is required. The p-value for the flexural strength and interlaminar shear strength can be increased in two ways, leading to a statistically significant result. First, additional panels with the same parameters could be produced and tested, increasing the sample population and lowering the variance. Second, further refinement of the manufacturing process could be done to reduce the standard deviation. The ILSS and flexural panels were created early in the year when the manufacturing process was less mature, it is expected that producing new panels with the existing processing capabilities would produce more consistent composites and reduce the standard deviation.

Table 17. P-Values from ANOVA for each mechanical test comparison.

| | p-value |
|-----------------------------|----------------|
| Flexural Strength | 0.00067 |
| Flexural Modulus | 0.64745 |
| Interlaminar Shear Strength | 0.00953 |
| Tensile Strength | 0.68225 |
| Tensile Modulus | 0.93163 |

Note: In bold are p-value that are above 0.05 significance level.

An ANOVA to compare the results between the 2D and 2.5D OTB test results was conducted and the results are displayed in Table 18. The recession rate, PHST, and average surface temperature had a p-value over 0.05 showing good results, but the p-values for the mass loss and char yield were lower than 0.05 indicating that further testing may be required. An ANOVA was not conducted between the molding compound and the 2D and 2.5D because the data were not available. A thorough ANOVA was conducted for the needle-punching experiments in Table 19. All combinations were tested included an ANOVA for all three experiments, 10 minute versus 20 minute, 10 minute versus 40 minute, and 20 minute versus 40 minute. All p-values for these results were above 0.05.

Table 18. P-Values from ANOVA for OTB tests on MC, 2D, and 2.5D.

| | 2D and 2.5D |
|------------------------------------|--------------------|
| Mass Loss | 0.01182 |
| Char Yield | 0.00576 |
| Recession Rate | 0.33441 |
| Peak Heat Soak Temperature | 0.59168 |
| Average Surface Temperature | 0.92084 |

Note: In bold are p-value that are above 0.05 significance level.

Table 19. P-Values from ANOVA for OTB tests on 10 min, 20 min, and 40 min.

| | All | 10 and 20 | 10 and 40 | 20 and 40 |
|------------------------------------|----------------|------------------|------------------|------------------|
| Mass Loss | 0.36981 | 0.22494 | 0.80534 | 0.25857 |
| Char Yield | 0.51080 | 0.34358 | 0.98607 | 0.30132 |
| Recession Rate | 0.62425 | 0.66004 | 0.69824 | 0.30579 |
| Peak Heat Soak Temperature | 0.28354 | 0.55849 | 0.08850 | 0.18660 |
| Average Surface Temperature | 0.16466 | 0.12698 | 0.23864 | 0.39174 |

Note: In bold are p-value that are above 0.05 significance level.

V. CONCLUSIONS

Material properties for a 2D laminate composite were compared with a needle-punched (2.5D) composite consisting of the same material system (polymer resin, fiber reinforcement, and density). Needle-punching enhanced the mechanical properties of the composite in flexural strength and interlaminar shear strength. Flexural tests show that the average flexural strength of the needle-punched composite was 28.8 MPa, compared to 10.27 MPa for the 2D composite, a 181% improvement. The interlaminar shear strength of the needle-punched and 2D composite was 2.62 MPa and 3.33 MPa, respectively, showing a 27% improvement. The tensile strength was not diminished by needle-punching, with the 2D composite presenting an 18.31 MPa and the 2.5D a 18.78 Mpa tensile strength.

Ablation performance is influenced by the robustness of the char layer, and the exceptional mechanical results indicate a composite that will have a higher resistance to delamination during ablation [8]. Comprehensive data were collected for the 2D and 2.5D composites and compared to MX-2600. In ablation testing, the 2.5D composites exhibited an improved recession rate, mass loss rate, and char yield when compared to the standard 2D composite. In mass loss, char yield, and PHST, the 2.5D composite outperformed the SOTA MX-2600 composite.

Ablation performance for three 2.5D composites was compared to understand the effect of needle-punching time on ablation performance. Increasing the needle-punching time from 10 minutes to 20 minutes visibly reduced delamination and improved the recession rate, mass loss, and char yield. Increasing the needle-punching to 40 minutes had a detrimental effect on all ablation parameters except PHST.

As shown in Table 20 below, it can be concluded that the affordable needle-punching and VARTM manufacturing methods are capable of producing an ablative composite that performs on par with the SOTA MX-2600. The final composite has mechanical properties (flexural and ILSS) that far-exceeded that of a 2D laminate and the negligible mechanical properties associated with a molding compound composite. In addition to performance and cost savings, the manufacturing techniques utilized provide a great deal of flexibility to rapidly change the shape of a composite with minimal tooling changes. This research demonstrates that further research into potential applications of this novel manufacturing method is warranted.

Table 20. Comparison of mechanical and ablation properties of MX-2600, 2D, and 2.5D [9] [22].

| | | Molding Compound | 2D | 2.5D |
|------------------------------|--|-------------------------------------|--|--|
| | Property | MX-2600 (SiO₂/Ph) | Woven and Non-woven SiO₂/Techneglas UHTR | Woven and Non-woven SiO₂/Techneglas UHTR |
| Materials and Process | Resin Type | MIL-R-9299, Type II phenolic resin | Techneglas UHTR | Techneglas UHTR |
| | Fiber | 19 ounce per yard silica fabric | 96% 8-harness woven silica fabric/100% silica non-woven | 96% 8-harness woven silica fabric/100% silica non-woven |
| | Processing | Custom mold in compression press | Vacuum infusion with oven curing | Vacuum infusion with oven curing |
| Mechanical | Interlaminar Shear Strength (Mpa) | Negligible mechanical properties | 2.62 | 3.33 |
| | Tensile Strength (Mpa) | | 18.31 | 18.78 |
| | Tensile Modulus (Gpa) (Modulus of Elasticity, MOE) | | 2.73 | 2.84 |
| | Flexural Strength (Mpa) | | 10.26 | 28.89 |
| | Flexural Modulus (Gpa) | | 3.89 | 3.96 |
| | Compressive Strength (Mpa) | | | |
| | Compressive Modulus (Gpa) | | | |
| Ablation | Heat-soaked Temperature (°C) | 360 | 252 | 303 |
| | Heat-soaked Time (s) | | 106 | 104 |
| | Recession Rate (mm/s) | 0.058 | 0.100 | 0.059 |
| | Mass Loss (%) | 31 | 41.2 | 27.7 |
| | Char Yield (%) | 69 | 58.8 | 72.3 |
| | Mass Loss Rate (g/s) | 0.031 | 0.049 | 0.031 |
| | Max Surface Temp (°C) | ~2,125 | 2,251 | 2,104 |
| | Average Surface Temp (°C) | ~2,050 | 2,084 | 2,242 |

APPENDIX SECTION

I. Technical Data Sheets



MX-2600

DESCRIPTION

MX-2600 is a nominal 19 ounce per square yard silica fabric impregnated with a MIL-R-9299, Type II phenolic resin containing silica filler. MX-2600 is available as a chopped molding compound in 1/8" x 1/8" squares.

PROPERTIES

Table 1 | Physical Properties

| Property | Nominal | Test Method |
|----------------------------|---------|-------------|
| Uncured | | |
| Resin Solids, % (Burn off) | 30 – 35 | R-111 |
| Flow at 2000 psi, % | 5 – 20 | F-84 |
| Bulk Factor | 4 – 7 | |
| Cloth % | 64 | R-162 |
| Filler % | 4.5 | R-162 |

Table 1 | Laminated Properties

Properties obtained when processed using the following cure cycle: 1000psi at 300-325°F for 30 minutes for 1/8" laminate. Alternate pressures have also been used successfully

| Property | Nominal | Test Method |
|---|---------|---------------|
| Cured | | |
| Tensile Strength, ksi | 7.6 | D-638 |
| Modulus, Msi | 2.9 | |
| Tensile Strength, ksi | 7.0 | D-651 |
| Flexural Strength, ksi | 14 | D-790 |
| Modulus, Msi | 2.2 | |
| Compressive Strength, ksi | 46 | D-695 |
| Modulus, Msi | 2.6 | |
| Interlaminar Dowel Shear, ksi | 9.9 | FTMS-406-1041 |
| Thermal Conductivity, BTU/in-hr-°F at 300°F | 0.23 | C-177 |
| Thermal Conductivity, BTU/in-hr-°F at 500°F | 0.22 | C-177 |
| Thermal Expansion Normal (ppm/°F) | 5 | D696 / D3386 |
| Thermal Expansion Parallel | 49 | D696 / D3386 |
| Hardness (Barcol) | 78 | D-2583 |
| Volatile Content, % (15 minutes at 325°F) | 2 – 6 | V-137 |
| Specific Gravity | 1.71 | D-792 |
| Mold Shrinkage, in/in | 0.0005 | D-551 |
| Specific Heat at 150°F | 0.27 | C-351 |
| Acetonic Extraction, % | 0.3 | D-494 |

www.cyttec.com

©2014 Cytec Industries Inc. • ASM-91 E3-EN Rev. 00 • 1 July 2014

Figure 44. MX-2600 data sheet [22]

Product Description

Dyna-Glas UHTR is a high solids resin system for high temperature FRP panel fabrication.

Application

Dyna-Glas UHTR resin system is used to prepare FRP composite panels that will be used in applications where temperatures range from 600°F to 1800°F. Dyna-Glas UHTR resin system does not require a post-cure cycle at, or above the anticipated service temperature of the fabricated parts. Dyna-Glas UHTR resin system may be used with common fiber reinforcements, including carbon, glass, silica and basalt.

Storage

The 'Best use before end' date of each batch is shown on the product label for non-catalyzed resin. Once catalyzed, pot life is 1-3 hours, depending on environmental conditions.

Recommended catalysts

Lower operating temperatures:

- Titanium (IV) Butoxide at 2-3 wt%

Higher operating temperatures

- N-(2-Aminoethyl)-3-aminopropyltrimethoxysilane at 1-2 wt%

Safety notes

Comprehensive instructions are given in the corresponding Material Safety Data Sheets which are available on request or at www.dyna-glas.com

| Product Data | |
|---|------------------------|
| Uncured Dyna-Glas UHTR | |
| Appearance | Slightly cloudy liquid |
| Viscosity | 95 cPs |
| Percent of Solids | 65% |
| Odor (liquid) | Slight Solvent |
| V.O.C. | 368 g/L |
| Specific Gravity | 1.05 |
| Pot Life at 25°C when catalyzed | 1-3 hours |
| Liquid Ignition Temperature | >300°C |
| Cured Dyna-Glas UHTR | |
| Appearance | Slightly yellow |
| Resin content of FRP | 40-50% |
| Density at 50% silica fiber | 1.6-1.7 g/mL |
| Thermal Conductivity | TBD |
| Flexural | TBD |
| Weight loss at 1000°C at 10°C/min (40°C/min) for neat resin | 14% (10%) |

Figure 45. Techneglas data sheet [23].



THE FINAL BARRIER AGAINST ABRASION, CHEMICALS AND HEAT

SILTEX® 18-UH AMORPHOUS SILICA CLOTH

SILTEX® 18-UH is a high performance fabric comprised of amorphous silica fibers woven into strong, flexible fabrics designed for use where severe temperature conditions exist. Manufactured to a finished weight of 18 ounces per square yard, the unique properties of SILTEX® 18-UH make it well suited for protection of personnel and equipment against moderate welding splatter, sparks, grinding of metals, etc. SILTEX® 18-UH is also excellent for use in engineered thermal insulation systems.



AVERAGE PHYSICAL PROPERTIES

| | |
|----------------------------------|-------------------------------|
| Material | 96% Amorphous Silica |
| Coating | Acrylic |
| Construction | Woven fabric, 8 harness satin |
| Use Limit | |
| Continuous | 1800° F • 982° C |
| Intermittent | 2300° F • 1260° C |
| Melting Point | 3100° F • 1704° C |
| Weight, oz/sy, nominal | 18 |
| Thickness, inches, nominal | .027 |
| Linear Shrinkage, % @ 30 minutes | <17 @ 1800° F • 982° C |
| Silica Content, % | 96 (+/- 1) |
| Width, inches, nominal | 36 (+/- 5%) |
| Packaging | 50 LY per roll, standard |
| | 300 LY master roll |

SILTEX® 18-UH is manufactured in accordance with MIL-C-24576.

Tolerance is +/- 10% unless otherwise stated.

The technical data presented herein are indicative of representative properties and are intended as a specification guide only. No warranties are expressed or implied as application conditions are beyond our control.

Rev. 2-10.5.2015



SILTEX® 18-UH Silica Cloth is ANSI/FM 4950 Approved for use in Welding Curtains.

Mid-Mountain Materials, Inc. • Telephone (800) 382-2208 • (206) 762-7600 • Fax (206) 762-7694
PO Box 800 • 2731 - 77th Avenue SE, Suite 100 • Mercer Island, WA 98040 USA
info@mid-mountain.com • www.mid-mountain.com

Figure 46. Woven silica data sheet [24].

Easy-to-handle SilcoSoft™ provides peak performance at high temperatures.

Soft, lightweight SilcoSoft™ is an advanced fiber with outstanding acoustical and thermal properties, providing top performance at temperatures as high as 2000° F (1200° C). Unlike other silica products, SilcoSoft features a unique cotton-like touch and easily conforms to irregular shapes. This remarkable material is non-dusting and non-irritating, and its 9 micron diameter fiber is non-respirable, which means handling SilcoSoft is safe and easy.

For more information and product samples, contact the BGF Sales Department at 1-800-476-4845, or visit our website at www.bgf.com.



SilcoSoft™
NONWOVEN MAT



SilcoSoft products are fabricated using 100% belCoTex® fiber produced in Germany by belChem Fiber Materials GmbH.

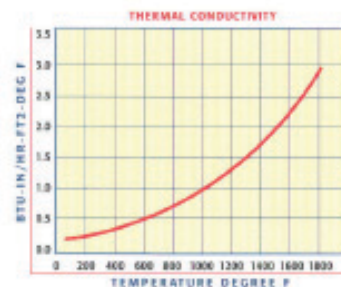
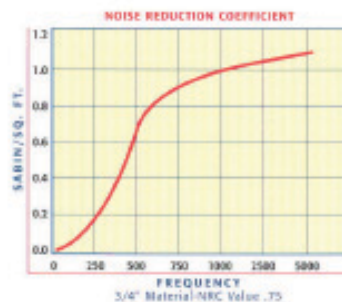


APPLICATIONS

- High temperature insulation
- Acoustical insulation
- Expansion joint and packing material
- Pre-heat furnace lining seals
- Pit cover and soaking linings
- Roller hearth furnace linings
- Kiln, furnace, boiler and incinerator linings
- Welding blankets
- Petrochemical process heater linings
- Heat-treating furnace linings
- Muffler packing
- Fire guard
- Mold wrap
- Valve and pipe insulation
- Catalytic converters
- Stress relieving pads
- Exhaust manifold insulation
- Liquid/gas filtration
- Insulating pads and blankets
- Nuclear insulation applications
- Glass furnace crown insulation repair

CHARACTERISTICS

- Withstands temperatures up to 2000° F (1200° C)
- Chemical resistant
- Excellent sound absorption
- Soft and fleecy fiber
- Non-respirable, 9 micron filament diameter
- Non-toxic
- Lightweight
- Easy handling



BGF Industries, Inc.

3802 Robert Poncher Way Greensboro, NC 27410
Ph: 336-545-0011 Fax: 336-545-0233
800-476-4845 sales@bgf.com

200

Figure 47. Non-woven silica brochure.

REFERENCES

1. Natali, M., J.M. Kenny, and L. Torre, *Science and technology of polymeric ablative materials for thermal protection systems and propulsion devices: A review*. Progress in Materials Science, 2016. **84**: p. 192-275.
2. Sutton, G.P. and O. Biblarz, *Rocket propulsion elements*. 8th;8. Aufl.;8; ed. 2010, Hoboken, N.J: Wiley.
3. Schellhase, K. J., Wu, H., Liu, E., Templin, T., Arguello, N., Head, L., . . . Brushaber, R. *Development of New Thermal Protection Systems Based on Silica/Polysiloxane Composites*. in *58th AIAA/ASCE/AHS/ASC Structures*. 2017. Grapevine, TX: AIAA.
4. Milos, F.S., *Galileo Probe Heat Shield Ablation Experiment*. Journal of Spacecraft and Rockets, 1997. **34**(6): p. 705-713.
5. Laub, B. and E. Venkatapathy. *Thermal Protection System Technology and Facility Needs for Demanding Future Planetary Missions*. in *International Workshop on Planetary Probe Atmospheric Entry and Descent Trajectory Analysis and Science*. 2003. Lisbon, Portugal.
6. SpaceX. *PICA Heat Shield*. 2013 [cited 2018 4/24]; Available from: <http://www.spacex.com/news/2013/04/04/pica-heat-shield>.
7. Koo, J.H., *Fundamentals, properties, and applications of polymer nanocomposites*. 2016, Cambridge: Cambridge University Press.
8. L. Torre, J. M. Kenny, G. Boghetich, and A. Maffezzoli, *Degradation behaviour of a composite material for thermal protection systems Part III Char Characterization*. Journal of Material Science, 2000. **35**: p. 4563– 4566.

9. K. J. Schellhase, J. H. Koo, H. Wu, and J. J. Buffy, *Experimental Characterization of Material Properties of Novel Silica/Polysiloxane Ablative*. AIAA Journal, 2018.
10. Strong, A.B., *Fundamentals of composites manufacturing: materials, methods and applications*. 2nd ed. 2008, Dearborn, Mich: Society of Manufacturing Engineers.
11. S. Meng, L. Song, C. Xu, W. Wang, W. Xie, and H. Jin, *Predicting the effective properties of 3D needled carbon/carbon composites by a hierarchical scheme with a fiber-based representative unit cell*. Composite Structures, 2017. **172**(Supplement C): p. 198-209.
12. X. Chen, L. Chen, C. Zhang, D. Zhang, and L. Song, *Three-dimensional needle-punching for composites – A review*. Composites Part A, 2016. **85**: p. 12-30.
13. L. M. Kumar, K. M. Usha, E. N. Anandapadmanabhan, and P. Chakravarthy, *Development of a Novel Ablative Composite Tape Layup Technology for Solid Rocket Motor Nozzle and Liquid Engine Liners*. Materials Science Forum, 2015. **830-831**: p. 417.
14. Boghazian, T., M. Stackpoole, and G. Gonzales, *Alternative High Performance Polymers for Ablative Thermal Protection Systems*. 2015.
15. Corporation, K. *Thermal - Heat Resistance | Characteristics of Fine Ceramics | FINE CERAMICS WORLD - All About Advanced Ceramics -*. 2017 [cited 2018 June 10]; Thermal: heat resistance]. Available from: <https://global.kyocera.com/fcworld/charact/heat/heatresist.html>.

16. Kumar, B.V.M. and Y.-W. Kim, *Processing of polysiloxane-derived porous ceramics: a review*. Science and Technology of Advanced Materials, 2010. **11**(4): p. 1-16.
17. Sinha, K. and S. Kumar, *Rocket Nozzle and its Manufacturing Methodologies*. 2009: Indian Institute of Space Science & Technology.
18. *Solid Rocket Motor Nozzles*, in *NASA Space Vehicle Design Criteria (Chemical Propulsion)*. 1975, National Aeronautics and Space Administration.
19. *PICA Material Property Report for Crew Exploration Vehicle Block II Heatshield Advanced Development Project (2009)*, in *NASA Report CEV TPS ADP, C-TPSA-A-DOC-158, Rev. 1*.
20. Schellhase, K.J., *Silica/Polysiloxane Ablative*. 2016: dyna-glas.com.
21. Corporation, V. *Thermogage | Inc*. 2018 [cited 2018 4/24]; Available from: <http://www.vatell.com/node/4>.
22. Cytec. *Layout 1 - MX-2600.pdf*. 2014 [cited 2017 April 25]; Available from: <https://www.cytec.com/sites/default/files/datasheets/MX-2600.pdf>.
23. Dyna-Glas. *DG-UHTR-PDS.pdf*. 2016 [cited 2017 April 15]; Available from: <http://www.dyna-glas.com/wp-content/uploads/2016/12/DG-UHTR-PDS.pdf>.
24. Mid-Mountain Materials, I. *SILTEX® 18UH - AR AMORPHOUS SILICA CLOTH*. [cited 2017 December 7]; Available from: <http://mid-mountain.com/wp-content/uploads/2013/08/Siltex-18-UH-AR.pdf>